

Test Results Prepared for Honeywell: Flammability of Refrigerants in the Japanese High Pressure Gas Law Test¹

Gregory T. Linteris, John Pagliaro, and Peter Sunderland
Fire Research Division
Building and Fire Research Laboratory
National Institute of Standards and Technology
Oct. 5, 2011

Introduction

The goal of the work was to determine the flammability of R1234ze(E) ($C_3H_2F_4$) per the Japanese High Pressure Gas Law (see Appendix I). Tests were also performed with R32 (CH_2F_2), R134a ($C_2H_2F_4$) and methane (CH_4), to provide a baseline for comparison of the results with R1234ze(E). Since the measured flammability of the mixture might be affected by the ignition source, tests were conducted with either copper wire (0.08 mm diameter) or the standard platinum wire (0.3 mm diameter). To aid in the interpretation of the experiments, calculations were also performed for the thermodynamic equilibrium conditions, the homogeneous autoignition time τ_{ign} , the overall chemical rate from stirred-reactor simulations, and the laminar burning velocity. These latter simulations employed a detailed chemical kinetic model, and solved the conservation equations for mass, energy, and species conservation.

Experimental Methods

The constant-volume combustion device is based on the Japanese High Pressure Gas Law (JHPGL), and is similar to the design of Takizawa [1], Shebeko [2], and others. The experimental apparatus is shown in Figure 1, while the plumbing and electrical schematics are shown in Figure 2 and Figure 3. The chamber consists of a stainless steel (316) sphere with an inner diameter of 15.24 cm, a volume of 1.85 L, and walls of 2.54 cm thickness; the vessel has nine tapped openings for gas inlet and outlet ports, and various transducers. Gases are introduced via the partial pressure mixing technique, and ignition is provided by a fused platinum or copper wire. As specified in the JHPGL, a thermocouple is located near the top of the chamber, and a rise in its temperature indicates ignition. While the JHPGL specifies a thermocouple of diameter 1 mm, the present device uses slightly smaller thermocouple to increase sensitivity by lowering the thermocouple time constant for heating. To increase the information provided by the experiment, a dynamic pressure transducer was also added, yielding the pressure as a function of time.

¹ Official contribution of NIST, not subject to copyright in the United States.

Initial sample gas composition was set using the method of partial pressure mixing via a digital strain gage transducer (Omega² DP80) with a range of 0 MPa to 1.33 MPa and a claimed accuracy of 13.3 kPa. The calibration of the pressure transducer was checked against two high-accuracy, Bourdon tube dial pressure gages (Heise Model CMM, 0.1 % of full scale accuracy, and against a Baratron 627D absolute pressure transducer), so that the uncertainty in the pressure reading is estimated to be 2 % of the reading. The sample gases were methane (Matheson Gas, UHP, 99.97 % purity), C₂H₂F₄ (Allied Signal, Genetron 134a), CH₂F₂ (R32, Honeywell), and C₃H₂F₄ (R1234ze(E), CHF=CHCF₃(trans), Honeywell). The air was house compressed air (filtered and dried) which is additionally cleaned by passing it through an 0.01 μm filter, a carbon filter, and a desiccant bed to remove small aerosols, organic vapors, and water vapor. The relative humidity of the dry shop air was measured with a humidity meter (TSI VELOCICALC model 8386), with a claimed accuracy of 3 % of the relative humidity reading. After mixing, the chamber gases settled for 5 min before ignition. The Initial temperature of the vessel was the room temperature, which was typically (22.4 ± 1) °C (but ranged from (21 ±1) °C to (25 ±1) °C).

For most tests a platinum wire igniter was used. This consisted of a 20 mm length of Pt wire, which was impulsively fused by a 100 V (AC) supply voltage. The igniter configuration was modified slightly from that recommended in the JHPGL. Rather than the igniter leads entering the chamber from two locations at right angles to each other, we used two parallel copper leads (57 mm long, 1 mm diameter) separated by 4 mm, with crimp-on connections (Digi-Key A34501-ND and A2161-ND) between the copper and platinum wires instead of welds. Hence, the igniter could be inserted through a single 0.25 inch fitting, with easily replaceable fusible wire. A variable transformer AC power supply (Powerstat, model 30N116C) supplied 100 VAC to the igniter, and its manual switch controlled ignition. The platinum wire melted and ruptured violently during each ignition process, and was replaced for each test. To explore the influence of the wire material, tests were also conducted with copper wire (20 mm length, 0.08 mm diameter) replacing the thicker, platinum wire.

A data acquisition system (DAS, National Instruments models NI USB-6259 and NI SCC-68, with Labview VI) connected to a personal computer (Dell GX-260) recorded the temperature and dynamic pressure during each experiment. The thermocouple (Omega, 0.81 mm diameter, stainless steel sheath capped, chromel-alumel, model 304-K-MO-032) was inserted in a fitting at the top of the chamber, and the tip was located 2.54 mm from the top inner surface of the chamber. A dynamic pressure sensor (PCB Piezotronics, model 101A06) with a range of 3450 kPa recorded the pressure rise in the

² Certain commercial equipment, instruments, or materials are identified in this paper to adequately specify the procedure. Such identification does not imply recommendation or endorsement by the National Institute of Standards and Technology, nor does it imply that the materials or equipment are necessarily the best available for the intended use.

chamber. The DAS collected data for 60 s at 100 Hz. Uncertainty in the temperature measurement is 1.5 K, and in the pressure measurement was 69 kPa.

Product gases were removed from the chamber at the end of each test to prevent product gas contamination for the subsequent test. Gaseous nitrogen was introduced to the chamber soon after the ignition: 1.) to quickly purge the chamber of the corrosive acid gases present for some experiments, and 2.) to reduce the temperature of the product gases (and thereby protect components from the potentially high product temperatures). After ignition, followed by a 10 s delay, gaseous nitrogen was supplied at 11 bar for 5 s before the exhaust valve was opened, whereby the N₂ flow continued for 1 min. After the nitrogen purge, the chamber was evacuated and maintained at about 12 kPa for 5 min. After that, clean and dried shop air was used to flush the chamber for two minutes. This process of evacuating the chamber and flushing with dry air was repeated twice. The experimental procedure developed for the present apparatus is given in Appendix II.

All³ uncertainties are reported as *expanded uncertainties*: ku_c , from a combined standard uncertainty (estimated standard deviation) u_c , and a coverage factor k . Likewise, when reported, the relative uncertainty is ku_c / X . The only measured parameters are the temperature, total pressure (static), dynamic pressure, and relative humidity. With a coverage factor of two, the uncertainty (type B) in the temperature is 1.5 K, and in the dynamic pressure, 69 kPa. For the total pressure (static), the relative uncertainty is 2 %, and for the relative humidity, 10 %.

Numerical Simulations

Numerical simulations were performed to compare the predicted overall chemical reactivity of each system with the results of the flammability limit tests. Simulations included premixed steady 1-D planar laminar flame speed, stirred reactor residence time just above blow-out, and homogeneous gas-phase ignition delay. The SANDIA numerical codes PREMIX [3], PSR [4], and SENKIN [5] were used, along with the chemical kinetics [6] and transport [7] interpreters.

Flame extinction is controlled by the characteristic times for chemical reaction and transport, as described by the Damköhler number $Da = \tau_r / \tau_c$, in which τ_r is the flow residence time, and τ_c is the chemical time [8]. Hence, an important step for understanding flame extinction is to obtain some measure of the overall reaction rate. The stirred-reactor blow-out residence time has been correlated with both the laminar flame speed [9] and with extinction of laminar diffusion flames with added inert

³ The policy of NIST is to provide statements of uncertainty for all original measurements. In this document however, data from organizations outside NIST are shown, which may include measurements in non-metric units or measurements without uncertainty statements.

suppressants [10], indicating its utility as a measure of overall reaction rate. The residence time in the reactor τ is defined as $\tau = \rho V / \dot{m}$, in which ρ is the mixture density, V is the reactor volume, and \dot{m} is the mass flow. Heat losses from the reactor to the surroundings can also be considered, but are neglected in the present analyses. The governing equations of conservation of mass, species, and energy form a system of coupled non-linear algebraic equations, which can be solved numerically. In the present work, we employ the SANDIA PSR code [4]. Initial pressure and temperature is 1.01 bar and 298 K.

To obtain the characteristic chemical time at extinction using a stirred-reactor model, one must determine the blow-out condition. The process is illustrated in Figure 4, which shows the reactor temperature as a function of residence time, for three values of the volume fraction of N_2 in the oxidizer. At a very low reactor mass flow, the residence time in the reactor is long, yielding the equilibrium conditions. As the mass flow in the reactor is increased, the temperature decreases slightly due to incomplete reaction, and there eventually becomes a point at which there is insufficient time to achieve substantial reaction in the vessel; because of the exponential dependence of reaction rate on temperature, this point is a very abrupt change, where the mixture “blows-out,” without reacting, yielding a blow-out time τ_{psr} . Near blow-out, a criterion of < 0.5 % change in the mass flow rate was used to determine τ_{psr} .

Kinetic Mechanism

A kinetic mechanism to describe the flames of methane, R32, R134a, and methane with added HFC-125 was assembled from sub-mechanisms available in the literature [11]. For the hydrocarbon mechanism, an optimized model for ethylene oxidation proposed by Wang and co-workers was employed [12,13], that included 111 species and 784 elementary reactions. This model has been optimized by considering experimental ignition delay and species profiles data from shock tubes, laminar flame speeds, species profile data from flow reactors, and species profile data from flat flames. To this mechanism, more detailed reactions of ethanol were added (5 species and 36 reactions), as proposed by Dryer and co-workers [14-16]. For the reactions of the hydrofluorocarbons (HFCs) in hydrocarbon flames, the National Institute of Standards and Technology (NIST) HFC mechanism was used [17,18]. Subsequent updates to that mechanism were made by NIST workers, as noted L’Espérance et al. [19]. Other changes to the NIST HFC mechanism were made in the present work based on recent experimental measurements and theoretical calculations [20-26] as listed in [19]. A list of potentially important reactions of C_2HF_5 with the radicals from initial fuel (propane or ethanol) decomposition was developed, and the rates were estimated as given in ref. [11]. The barriers for the reactions were estimated in Evans-Polanyi fashion by analogy to that for the reference reaction $CHF_2-CF_3 + CH_3 = CF_3-CF_2 + CH_4$ contained in the NIST HFC mechanism by increasing the barriers in proportion (0.3) to the decrease in the heat of reactions relative to the reference reaction. The HFC sub-mechanism finally

adopted contained 51 species and 600 reactions. The final mechanism used for the simulations had 177 species and 1494 reactions.

Results and Discussion

Experimental

Temperature and pressure rise data were collected for experiments with methane, R32, R134a, and R1234ze(E) as fuels. The lean and rich flammability limits were examined by performing tests over a range of agent partial pressures near the published flammability limits. Typical time histories of the measured thermocouple temperature and pressure are shown in Figure 5 for methane and R32, each at three initial fuel partial pressures. The peak values are determined from curves similar to those in Figure 5, and are reported for each compound below. Raw data for all of the tests are given in Appendix III.

Igniter Characterization

Ignition tests were also conducted with air or nitrogen in the chamber (i.e., no added refrigerant) to assess the temperature rise from the ignition event itself. With nitrogen or air, the peak temperature rise of the thermocouple was 3.9 K or 10.3 K, respectively, and the peak pressure rise was 0.074 bar or 0.078 bar. While the thermocouple is likely heated by a bubble of hot gases rising to meet it, we can estimate a rough upper limit of the energy added to chamber air by assuming the entire volume chamber air is heated to the peak temperature indicated by the temperature bead. Doing this gives 9 J and 23 J for the tests with nitrogen or air in the chamber, respectively.

To put some bounds on the energy added to the system by melting the platinum or copper wire, the sensible and latent heat the materials brought to a liquid state were calculated. The material properties are listed in Table 1. While we do not know that the wire heats evenly, we present a calculation in which the sensible heating is assumed to occur uniformly over the entire length of the wire, and the fraction of the wire which melts is preserved as a variable. Figure 7 shows the energy required to melt the copper or platinum igniter wire. As indicated, the copper wire requires between about 0.4 J and 0.56 J, while the platinum wire requires about 7 J to 10 J (both for 0 % to 100 % of the wire melted). Of course, this number can be greater if the metal superheats before the connection is severed. While it might be fortuitous, the value for platinum (7 J to 10 J) is of the same order as the upper limit of the energy rise in the nitrogen in the chamber (9 J). These energies are orders of magnitude larger than those typically used in spark ignition experiments of hydrocarbon/air mixtures [27].

Methane

Figure 6 shows the peak temperature rise of the thermocouple (\diamond , left axis) and the peak pressure rise measured by the dynamic pressure transducer (\square , right axis), as a function

of the CH₄ initial partial pressure. (The lines in the figure connect data points, and are intended to aid the reader.) Note that since the compressibility of all the fuels tested here is very small at the initial pressures (≈ 1 bar), the fuel partial pressure is indistinguishable from fuel volume fraction. The traditional CH₄-air flammability limits [28] are given by the vertical green lines at 5 % and 15 % initial CH₄ partial pressure fraction. To determine a flammability limit using the JHPGL, one would need a criterion for the temperature rise; as given in Appendix I, the stated criterion is: *“If it is determined, by means of the temperature change within the explosion vessel (a), that the gas therein has ignited, then an explosion is deemed to have occurred.”* The ability of the JHPGL to reproduce the traditional methane-air flammability limits (determined using the Bureau of Mines flammability tube test [29]) appears to be dependent upon the criterion used for the temperature rise. For example, with a criterion of 210 K, the lean limit would be about 5 %, while the rich limit would be about 17 %; however, a criterion of 50 K would give a lean limit of 4.5 % and a rich limit of about 25 %. For the rich flames, rather than a steep drop in the temperature rise beyond the flammability limits, there is a long tail, extending out past 25 %. The pressure rise shows similar behavior.

The platinum wire subjected to the input voltage of 100 VAC, as specified in the JHPGL test, causes an explosive destruction of the wire. The remnants of the igniter are shown in Figure 8, which shows the inside top surface of the chamber after a few tests with the platinum igniter. As illustrated, there were hardened spheres of platinum, forming a spray pattern, consistent with the plane of the platinum wire before it was energized. Since platinum is a catalyst for combustion reactions, it is not surprising that spraying the reactants with molten platinum droplets creates wider flammability limits than do the low-energy sparks used in flammability tube tests.

To explore the influence of the igniter on the flammability limits, we also ran tests with a 40 gage (0.08 mm diameter) copper wire, also subjected to 100 VAC. The results are shown in Figure 6 by the orange squares and diamonds. The copper igniter reproduces the traditional CH₄-air limits very well, highlighting the overdriven nature of the JHPGL platinum wire test procedure.

R32

The pressure and temperature rise data in the 2-L chamber for R32 (CH₂F₂) are shown in Figure 9, together with the flammability limits determined by Kondo et al. [30]. Again, the limits in the present device are somewhat wider than others—in this case, those of Kondo et al. For this fuel, the widening of the limits, relative to the other tests, is about equal on the rich and lean sides. As with methane, the pressure and temperature measurements yield similar flammability limits.

R1234ze(E)

The pressure and temperature rise in the 2-L chamber for R1234ze(E) ($C_3H_2F_4$) is shown in Figure 10, together with the flammability limits (at 40° C) as provided by Honeywell [31]. The results are similar to those of CH_4 -air: the lean limit is about the same as obtained in the Honeywell experiments, while the rich limit is wider and falls off less steeply than the lean limit. For $C_3H_2F_4$, the pressure rise measurement provides qualitatively the same results, with perhaps slightly narrower flammability limits.

Test with R1234ze(E) were also conducted with the copper wire igniter. The results are shown by the orange squares in Figure 10. As indicated, there was no significant temperature or pressure rise. Clearly, the results with the platinum wire are different for this fuel.

R134a

In order to explore the flammability limits of another well-studied refrigerant in the JHPGL test, experiments were performed with R134a ($C_2H_2F_4$), as indicated in Figure 11. The solid symbols refer to tests with dry air (1 % RH to 3 % RH), while the open symbols refer to conditions at 57 % RH \pm 2 % RH. All tests were performed using platinum wire. Both the temperature and pressure rise are minimal, below any temperature or pressure rise criteria which would indicate a successful ignition event in the tests with methane, R32, or R1234ze(E). The tests at higher relative humidity were performed for R134a because of the higher reactivity predicted in the stirred reactor simulations for 100 % RH, as described below. While they did show a larger temperature and pressure rise at a $C_2H_2F_4$ partial pressure of 8.5 %, it was not nearly as large as expected based on the PSR simulations, and at a $C_2H_2F_4$ partial pressure of 12 %, the more humid conditions had smaller pressure and temperature rise.

Numerical

Methane

The characteristic chemical rate, as determined by the calculated PSR blow-out condition, is shown in Figure 12 as a function of the methane volume fraction for methane-air mixtures. Also shown is the PSR temperature at blow-out T_{psr} , the adiabatic equilibrium temperature T_{ad} , and the laminar burning velocity S_L . As illustrated, both the stirred reactor chemical time and the burning velocity correlate reasonably well with the flammability limits. Interestingly, the laminar flame speed has a tail on the rich side, similar to the temperature or pressure rise measured in the JHPGL

Figure 13 shows the calculated ignition delay τ_{ign} for homogeneous mixtures of methane-air at initial temperatures of 1400 K and 1500 K, as a function of the fuel-air equivalence ratio ϕ . As shown, the ignition delay does not capture the variation in the

flammability with ϕ , implying that the chemistry important for homogeneous auto-ignition is not that relevant for flammability limits. This is further illustrated in Figure 14, which shows the ignition delay for methane, R32, and R134a with air as a function of ϕ . A comparison of Figure 13 with Figure 12 shows that variation in τ_{ign} with ϕ is incorrect; further, Figure 14 shows that the trend in τ_{ign} with fuel type (R134a < R32 < methane) is opposite the order of flammability (methane > R32 > R134a).

R32

For R32 with air (50 % RH), Figure 15 shows the characteristic chemical rate ω_{psr} calculated from the PSR simulation, the laminar burning velocity S_L , and the equilibrium and PSR temperatures. The blue lines indicate the flammability limits determined by Kondo et al. [30]. As the figure shows, the trends predicted by the PSR and burning velocity simulations are correct, but the predicted flammability is shifted somewhat toward leaner flames than observed in the experiments. It should be noted that the NIST HFC mechanism was developed for small concentrations of HFCs added to hydrocarbon flames (to examine hydrocarbon flame inhibition by HFC fire suppressants)—not for pure flames of HFCs with air; hence, there may be important reaction routes in the present chemical systems not accounted for in the NIST HFC mechanism. It is noteworthy, however, that the PSR and burning velocity simulations predict similar behavior for R32-air.

R134a

For R134a with air, Figure 16 shows the characteristic chemical rate ω_{psr} calculated from the PSR simulation and the equilibrium T_{ad} and PSR T_{psr} temperatures. As shown, the PSR simulations predict a strong dependency of the overall chemical rate, as well as the temperature in the PSR, on the humidity of the air. To test this predicted trend, we conducted experiments with R134a at 2 % RH and 57 % \pm 2 % RH. In the 2-L chamber tests, there was some effect of the humidity on the ignition trends at R134a partial pressures of 8.6 % and 12 %, the pressure rise never went above 0.2 bar, and the thermocouple temperature rise did not go above 23 K. The discrepancy between the PSR simulation and the 2-L chamber experiment may be due to shortcomings in the kinetic mechanism for 134a.

R125

In order to further test the utility of PSR simulations for understanding flammability limits, we performed calculations for methane-air-C₂HF₅ mixtures. For comparison with the simulations, we used the flammability map data of Kondo et al. [1] as shown in Figure 17 (inside the curve is flammable, outside is not). The predicted overall chemical rate in the PSR ω_{psr} is shown in Figure 18 (z-axis) with the flammability contour

determined by Kondo et al. on the horizontal surface. The lines across the map are for values of constant $R=X_{R125}/(X_{R125}+X_{CH4})$, in which X_{R125} and X_{CH4} are the volume fraction of HFC-125 and CH_4 . In Figure 19, the same data of Figure 18 are plotted in 2-D, with different curves representing the different values of R. As shown by Figure 18 and Figure 19, the PSR simulation does a reasonable job of predicting the flammability limits for this chemical system.

Conclusions

The behavior of methane, R32, R1234ze(E), and R134a have been investigated through constant-volume combustion experiments that closely approximate the Japanese High Pressure Gas Law (JHPGL). The flammability limits defined by the present tests are dependent upon the temperature rise criterion specified in the JHPGL, which is not quantitative. When using the specified platinum igniter wire, the indicated flammability limits for R32 and methane were somewhat wider in the JHPGL than in other experiments, particularly for methane on the rich side of stoichiometric. For methane-air flames, experiments with thinner copper wire, rather than thicker platinum wire, gave narrower flammability limits which are closer to those published for the classic Bureau of Mines flammability tube (Coward and Jones) with weak spark ignition. For R1234ze(E), the tests with the copper igniter did not show flammability, while those with the platinum igniter gave flammability limit values consistent with the limits provided by Honeywell (and once again, the exact flammability limits in the present tests will depend upon the temperature rise criterion selected). For R134a, tests with the platinum igniter and dry air gave a maximum peak temperature rise of 21.6 K; hence, any temperature rise criterion above 22 K would indicate no ignition. Pressure rise was also measured, and gave results qualitatively the same as the temperature rise. In the present experiment, the apparent flammability of the refrigerants with air depends upon both the criterion for the temperature rise, and the type of igniter used.

To aid in the understanding of the chemical systems, numerical simulations were performed, for thermodynamic equilibrium conditions, homogeneous auto-ignition, stirred-reactor blow-out conditions, and laminar burning velocity. Detailed numerical simulations were performed for air (with trace water vapor) for methane, R32, R134a, and R125 systems using a chemical mechanism with 177 species and 1494 reactions. The adiabatic equilibrium temperature, stirred-reactor temperature at blow-out, and the homogeneous ignition delay did not correlate with the measured flammability limits. However, both the burning velocity and the characteristic chemical reaction rate determined with the stirred-reactor simulations correlated reasonably well with the measured flammability limits.

References

- [1] S.Kondo, K.Takizawa, A.Takahashi, K.Tokuhashi, A.Sekiya, *Fire Safety Journal* 44 (2009) 192-197.
- [2] Y.N.Shebeko, V.V.Azatyanyan, I.A.Bolodian, V.Y.Navzenya, S.N.Kopyov, D.Y.Shebeko, E.D.Zamishevski, *Combustion and Flame* 121 (2000) 542-547.
- [3] A Fortran Computer Program for Modeling Steady Laminar One-Dimensional Premixed Flames, SAND85-8240, Sandia National Laboratories, 1991.
- [4] P.Glarborg, R.J.Kee, J.F.Grcar, J.A.Miller, PSR: A FORTRAN Program for Modeling Well-Stirred Reactors, SAND86-8209, Sandia National Laboratories, 1986.
- [5] SENKIN: A Fortran Program for Predicting Homogeneous Gas Phase Chemical Kinetics With Sensitivity Analysis, SAND87-8248, Sandia National Laboratories, 1988.
- [6] CHEMKIN-II: A Fortran Chemical Kinetics Package for the Analysis of Gas Phase Chemical Kinetics, SAND89-8009B, Sandia National Laboratories, 1989.
- [7] A Fortran Computer Package for the Evaluation of Gas-Phase, Multicomponent Transport Properties, SAND86-8246, Sandia National Laboratories, 1986.
- [8] F.A.Williams, *Journal of Fire and Flammability* 5 (1974) 54-63.
- [9] R.B.Barat, *Chemical Engineering Science* 56 (2001) 2761-2766.
- [10] S.Liu, M.C.Soteriou, M.B.Colket, J.A.Senecal, *Fire Safety Journal* 43 (2008) 589-597.
- [11] G.T.Linteris, D.R.Burgess, V.R.Katta, F.Takahashi, H.K.Chelliah, O.Meier, *Combust Flame* accepted (2011) xxx.
- [12] D.A.Sheen, X.Q.You, H.Wang, T.Lovas, *Proceedings of the Combustion Institute* 32 (2009) 535-542.
- [13] H.Wang, X.You, K.W.Jucks, S.G.Davis, A.Laskin, F.Egolfopoulos, C.K.Law, USC Mech Version II. High-Temperature Combustion Reaction Model of H₂/CO/C₁-C₄ Compounds, http://ignis.usc.edu/USC_Mech_II.htm, University of Southern California, 2007.

- [14] J.Li, A.Kazakov, M.Chaos, F.L.Dryer, in: Proceedings of the Fifth Joint Meeting of the U.S.Sections of The Combustion Institute, Combustion Institute, 2007, p. Paper 26.
- [15] J.Li, A.Kazakov, F.L.Dryer, International Journal of Chemical Kinetics 33 (2001) 859-867.
- [16] J.Li, A.Kazakov, F.L.Dryer, Journal of Physical Chemistry A 108 (2004) 7671-7680.
- [17] D.R.Burgess, M.R.Zachariah, W.Tsang, P.R.Westmoreland, Progress in Energy and Combustion Science 21 (1995) 453-529.
- [18] D.Burgess, M.R.Zachariah, W.Tsang, P.R.Westmoreland, Thermochemical and Chemical Kinetic Data for Fluorinated Hydrocarbons, NIST Technical Note 1412, National Institute of Standards and Technology, 1995.
- [19] D.L'esperance, B.A.Williams, J.W.Fleming, Combust. Flame 117 (1999) 709-731.
- [20] Y.Saso, D.L.Zhu, H.Wang, C.K.Law, N.Saito, Combustion and Flame 114 (1998) 457-468.
- [21] K.Takahashi, Y.Sekiuji, Y.Yamamori, T.Inomata, K.Yokoyama, Journal of Physical Chemistry A 102 (1998) 8339-8348.
- [22] Y.Yamamori, K.Takahashi, T.Inomata, Journal of Physical Chemistry A 103 (1999) 8803-8811.
- [23] B.Vetters, B.Dils, T.L.Nguyen, L.Vereecken, S.A.Carl, J.Peeters, Physical Chemistry Chemical Physics 11 (2009) 4319-4325.
- [24] A.Fernandez, A.Fontijn, Journal of Physical Chemistry A 105 (2001) 8196-8199.
- [25] C.P.Tsai, D.L.Mcfadden, Journal of Physical Chemistry 94 (1990) 3298-3300.
- [26] J.S.Francisco, Journal of Chemical Physics 111 (1999) 3457-3463.
- [27] S.D.Tse, D.L.Zhu, C.K.Law, Review of Scientific Instruments 75 (2004) 233-239.
- [28] I.Glassman, Combustion, Academic Press, San Diego, CA, 1996.
- [29] H.F.Coward, G.W.Jones, Limits of Flammability of Gases and Vapors, AD0701575, US bureau of Mines, 1952.
- [30] S.Kondo, Y.Urano, K.Takizawa, A.Takahashi, K.Tokuhashi, A.Sekiya, Fire Safety Journal 41 (2006) 46-56.

[31] R.G.Richard, Personal Communication, 2011.

Table 1 - Properties of platinum and copper igniter wires.

Wire Material	Platinum	Copper
Diameter (mm)	0.3	0.08
Length (mm)	20	20
mass (g)	3.03E-05	9.00E-07
Melting Point (K)	2041.4	1357.8
Cp (kJ/kg/K)	0.13	0.39
Heat of Fusion (KJ/mol)	22.17	13.26



Figure 1 - 2-L chamber.

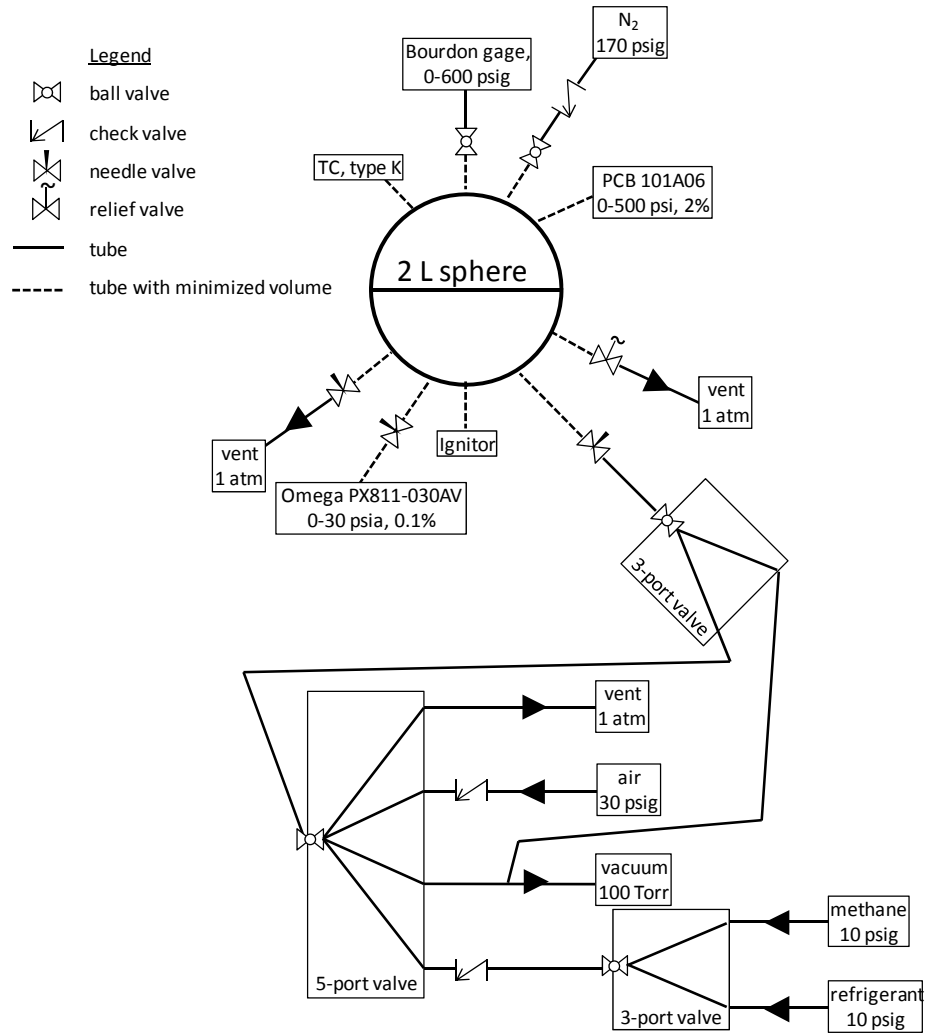


Figure 2 - Plumbing schematic diagram of 2-L chamber.

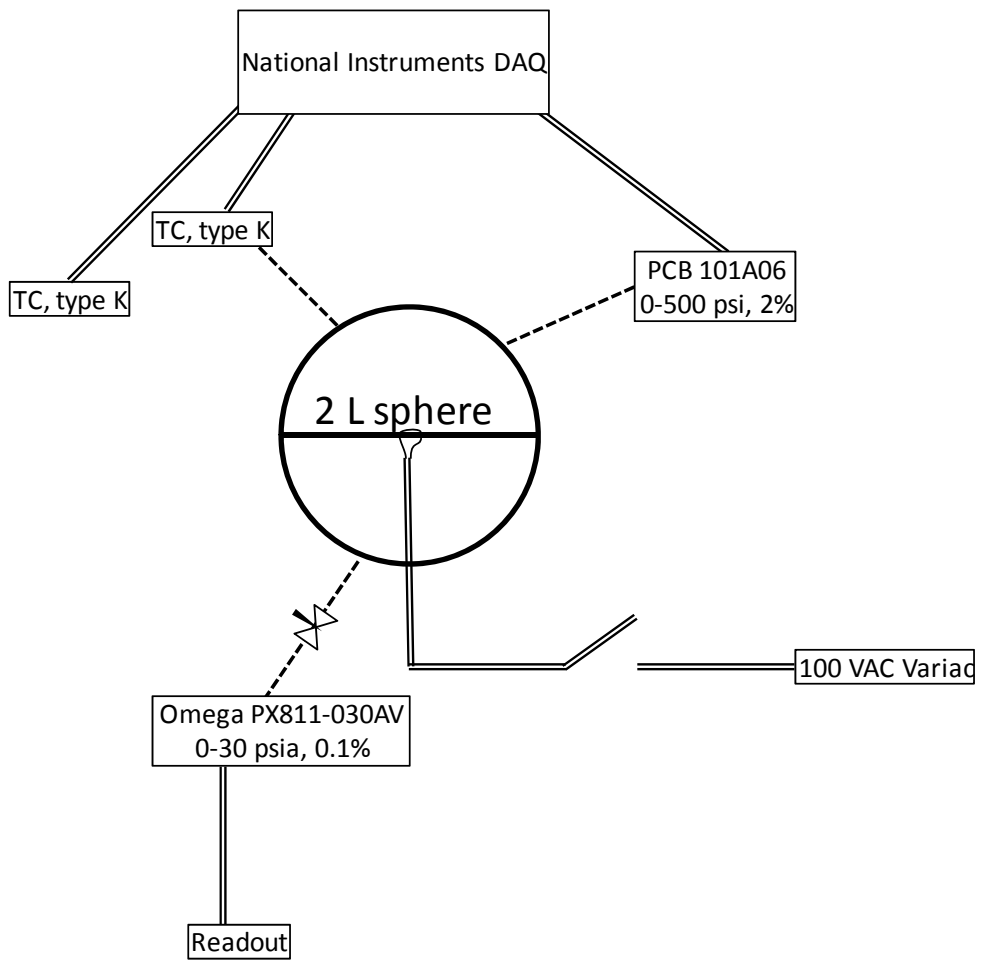


Figure 3 - Electrical schematic diagram of 2-L chamber.

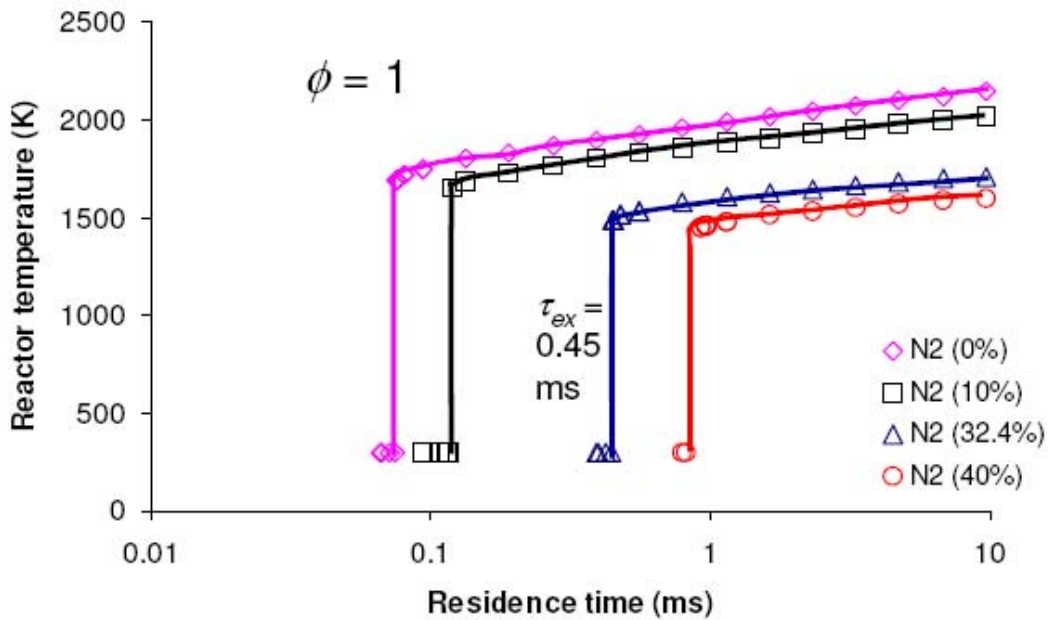


Figure 4 - Stirred reactor temperature as a function of residence time for a stoichiometric methane-air system with added N₂ suppressant at volume fractions of 0, 0.1, 0.32, and 0.4 (from [10]).

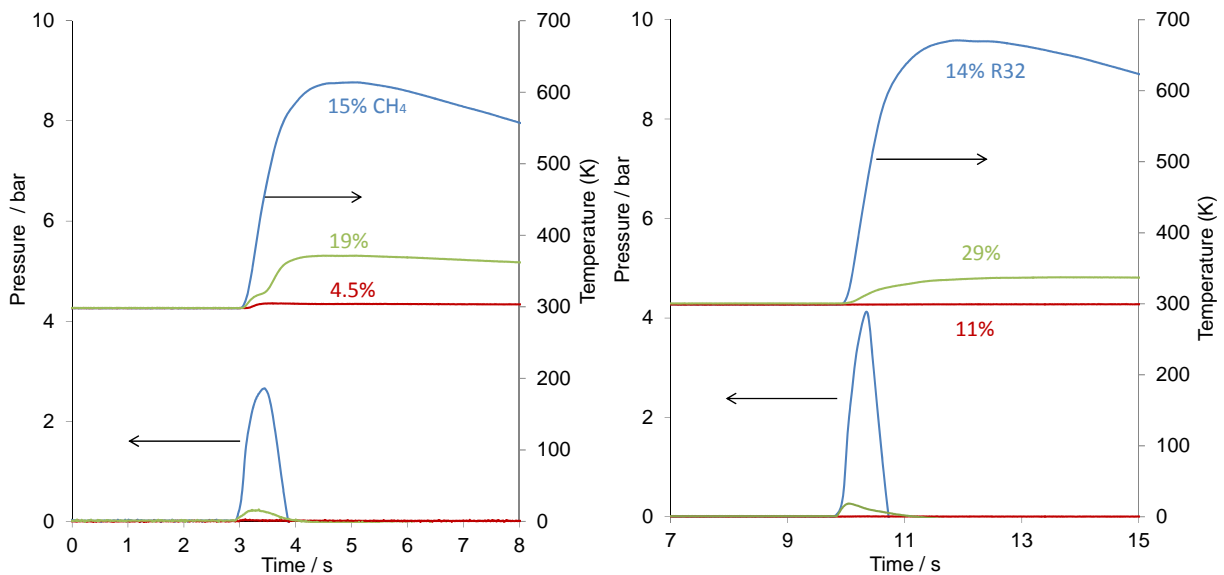


Figure 5 - Thermocouple temperature and dynamic pressure measurements as a function of time for methane (left frame) and R32 (right frame); the different curves refer to non-flammable (red), marginally flammable (green), and flammable mixtures (blue).

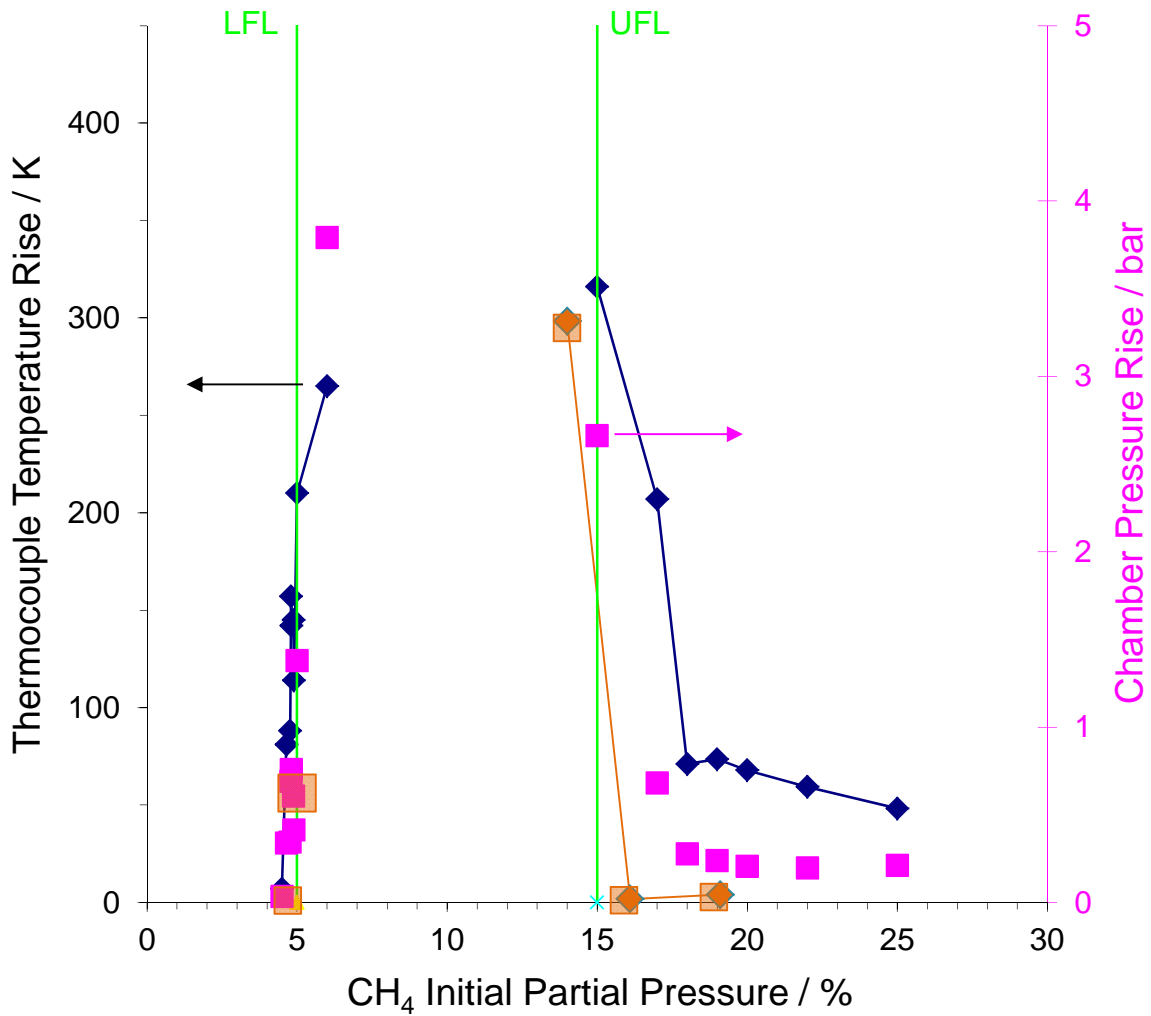


Figure 6 - Thermocouple temperature rise and chamber pressure rise with CH₄ - air mixtures in 2-L vessel. Vertical green lines show the lower and upper flammability limits (from ref. [28]).

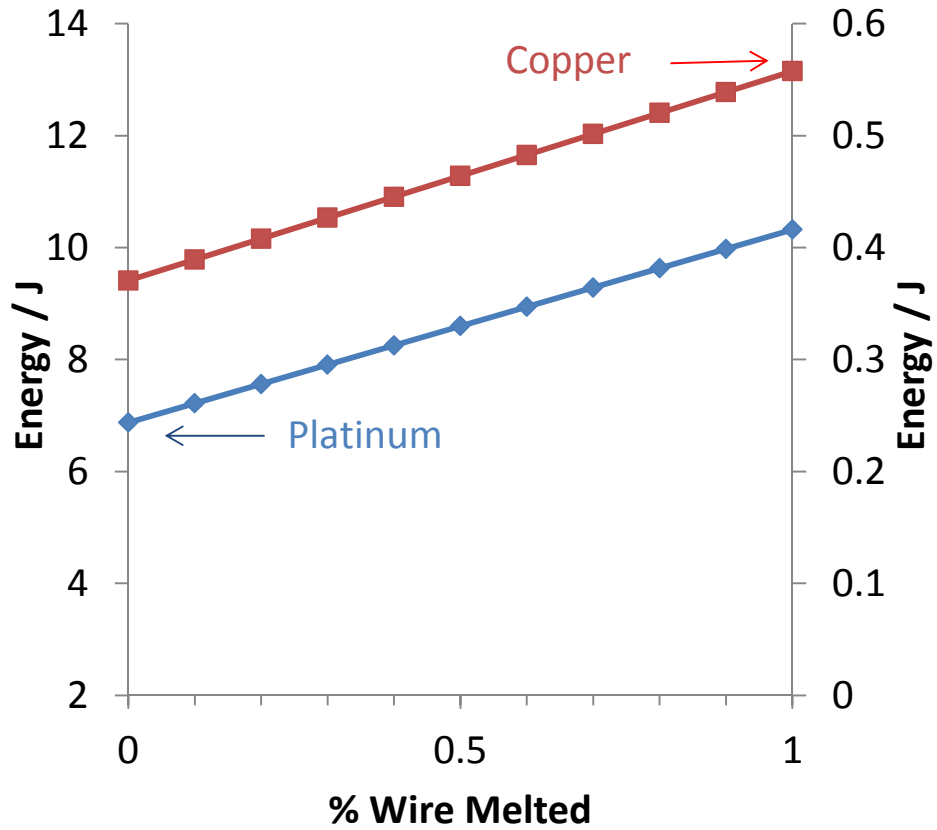


Figure 7 - Energy required to melt the copper or platinum wires in the present experiment as a function of the fraction of igniter melted.



Figure 8 - Top, inside surface of 2-L chamber after several tests with the platinum igniter.

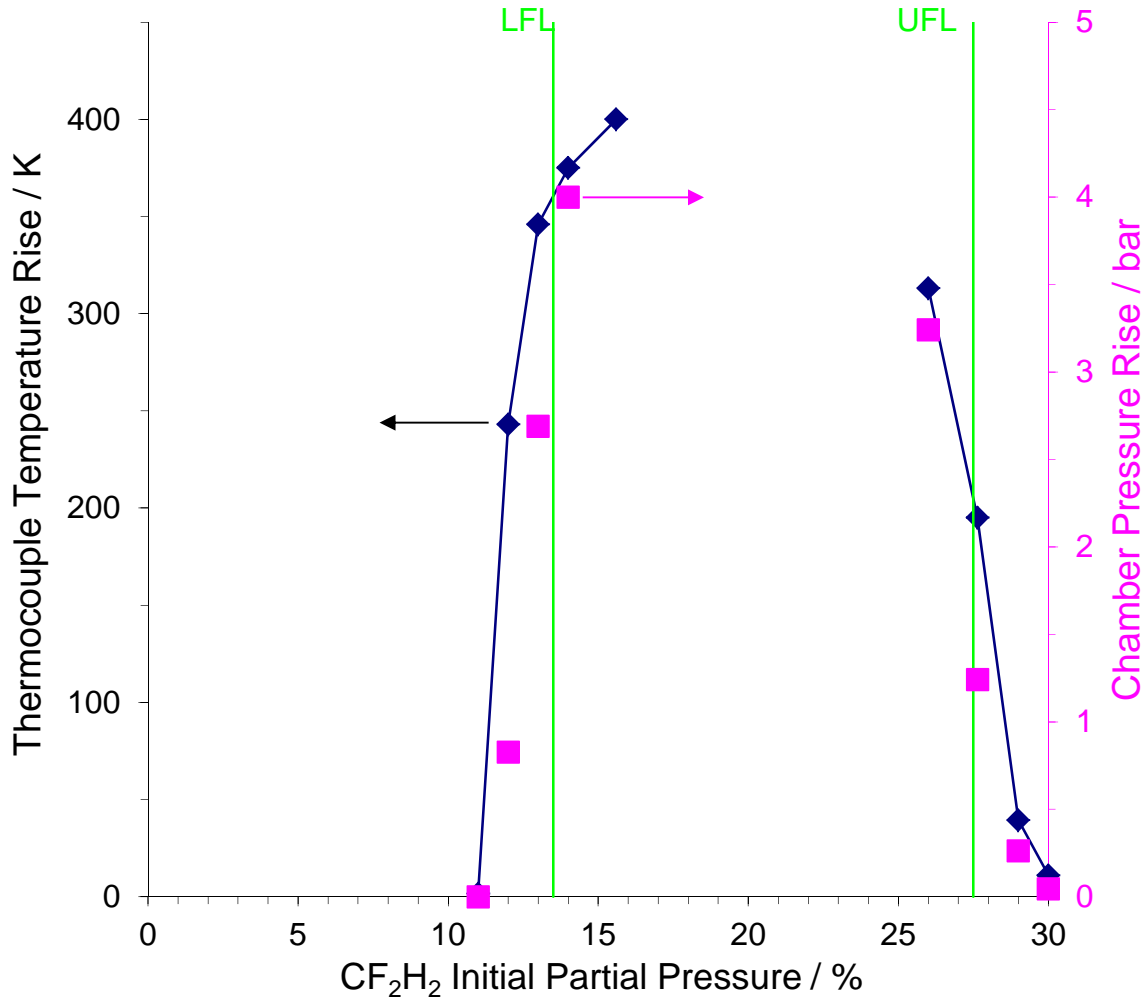


Figure 9 - Thermocouple temperature rise and chamber pressure rise with CH_2F_2 - air mixtures in 2-L vessel. Vertical green lines show the lower and upper flammability limits (from ref. [30]).

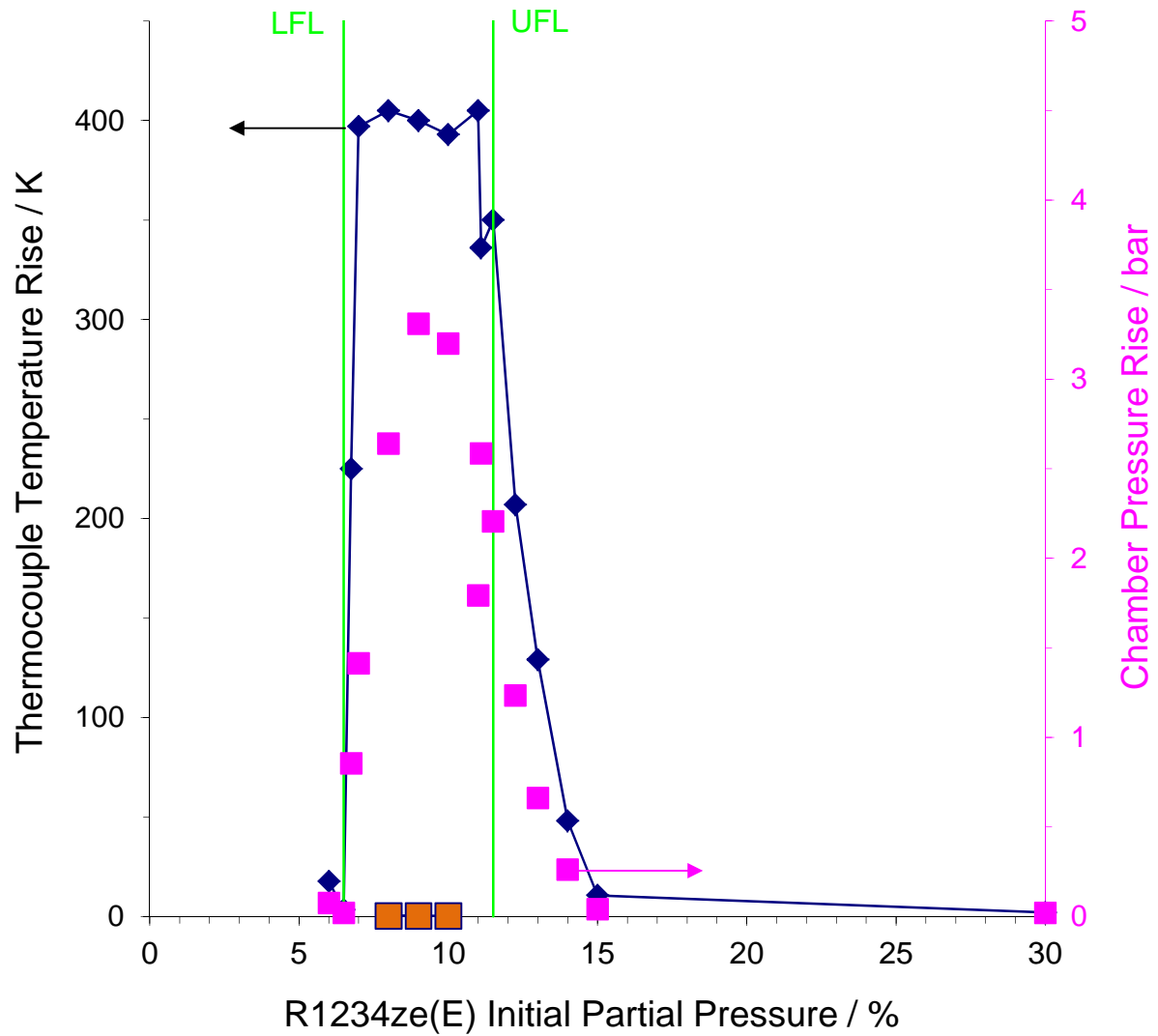


Figure 10 - Thermocouple temperature rise and chamber pressure rise with $C_3H_2F_4$ - air mixtures in 2-L vessel. Vertical green lines show the lower and upper flammability limits.

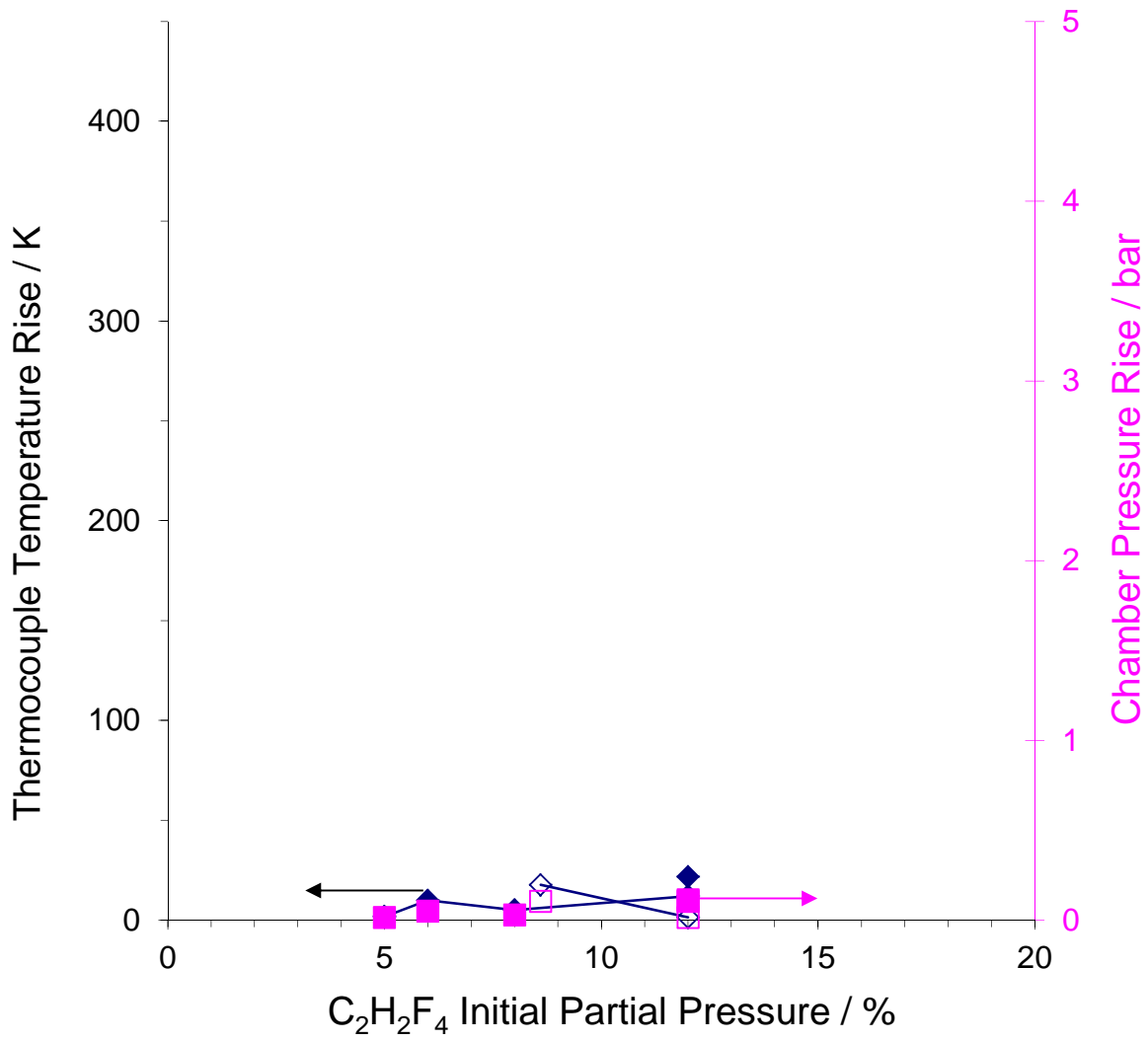


Figure 11 - Thermocouple temperature rise and chamber pressure rise with R134a - air mixtures in 2-L vessel.

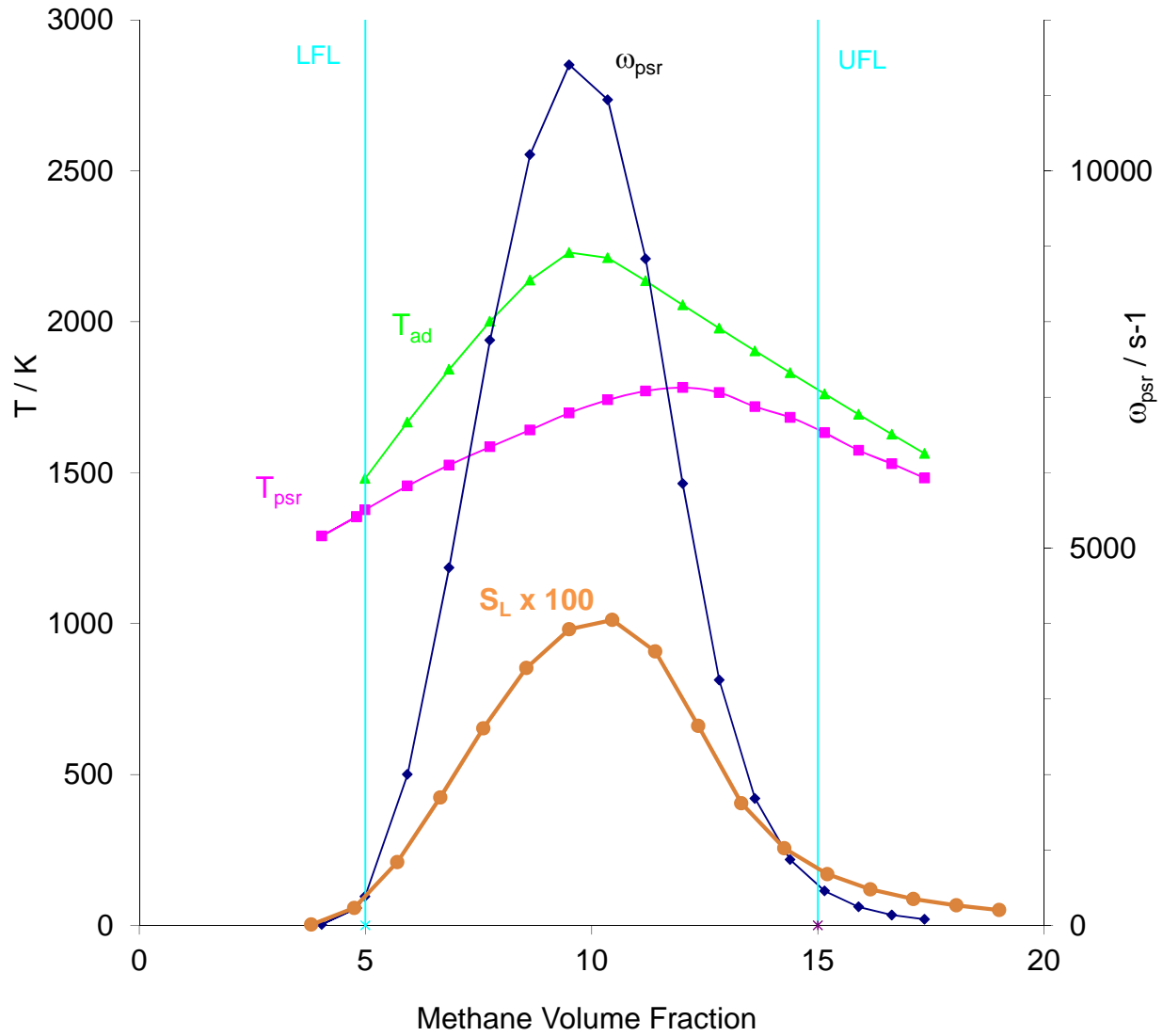


Figure 12 - PSR predictions of overall chemical rate ω_{psr} and laminar flame speed S_L (right scale), and equilibrium adiabatic temperature and PSR temperature (left scale) for methane-air mixtures.

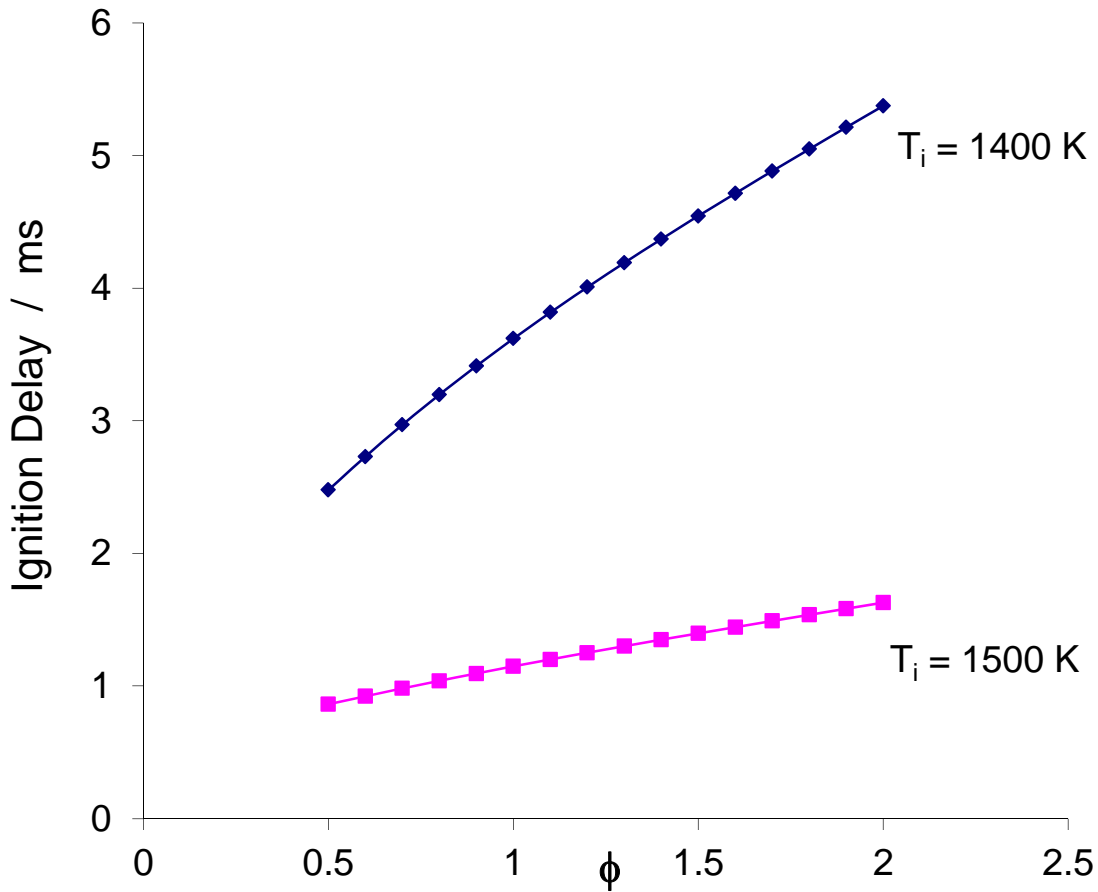


Figure 13 - Homogeneous ignition delay for methane-air mixtures at 1400 K and 1500 K initial temperature.

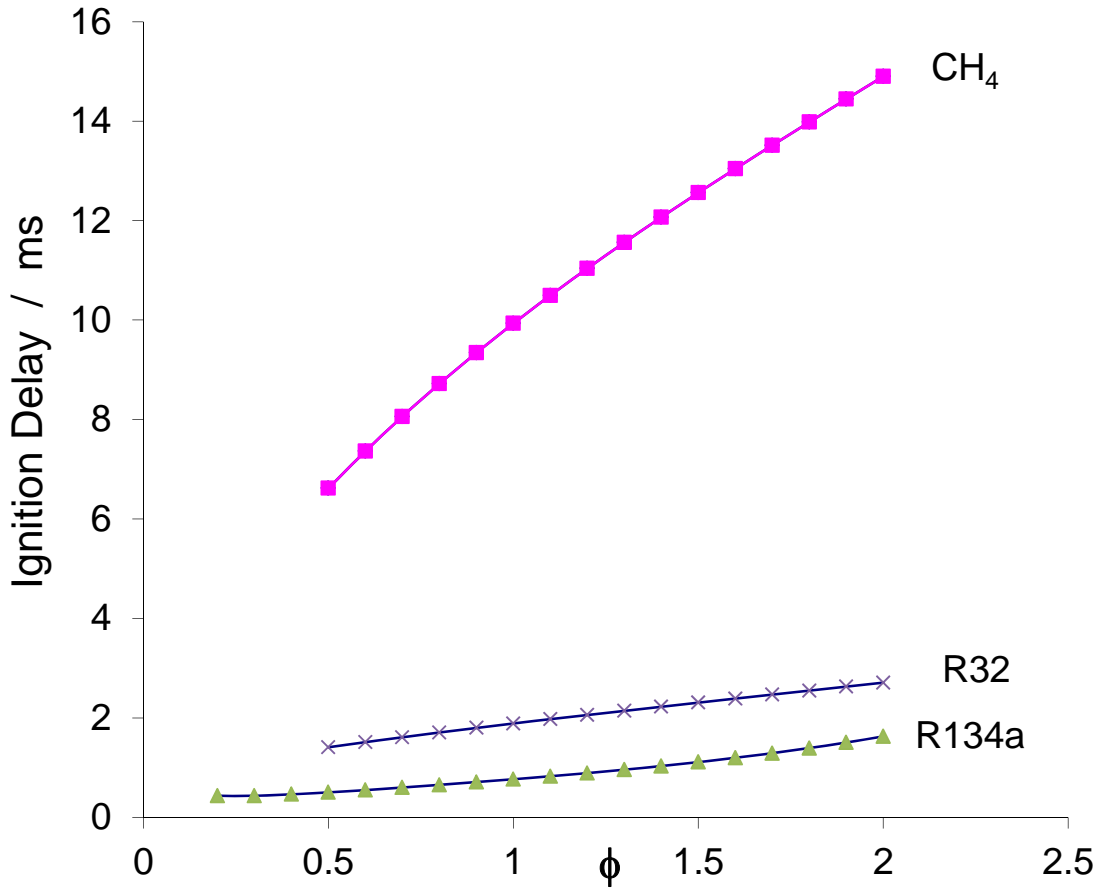


Figure 14 - Homogeneous ignition delay for methane-air, R32-air, and R134a-air mixtures at 1320 K initial temperature.

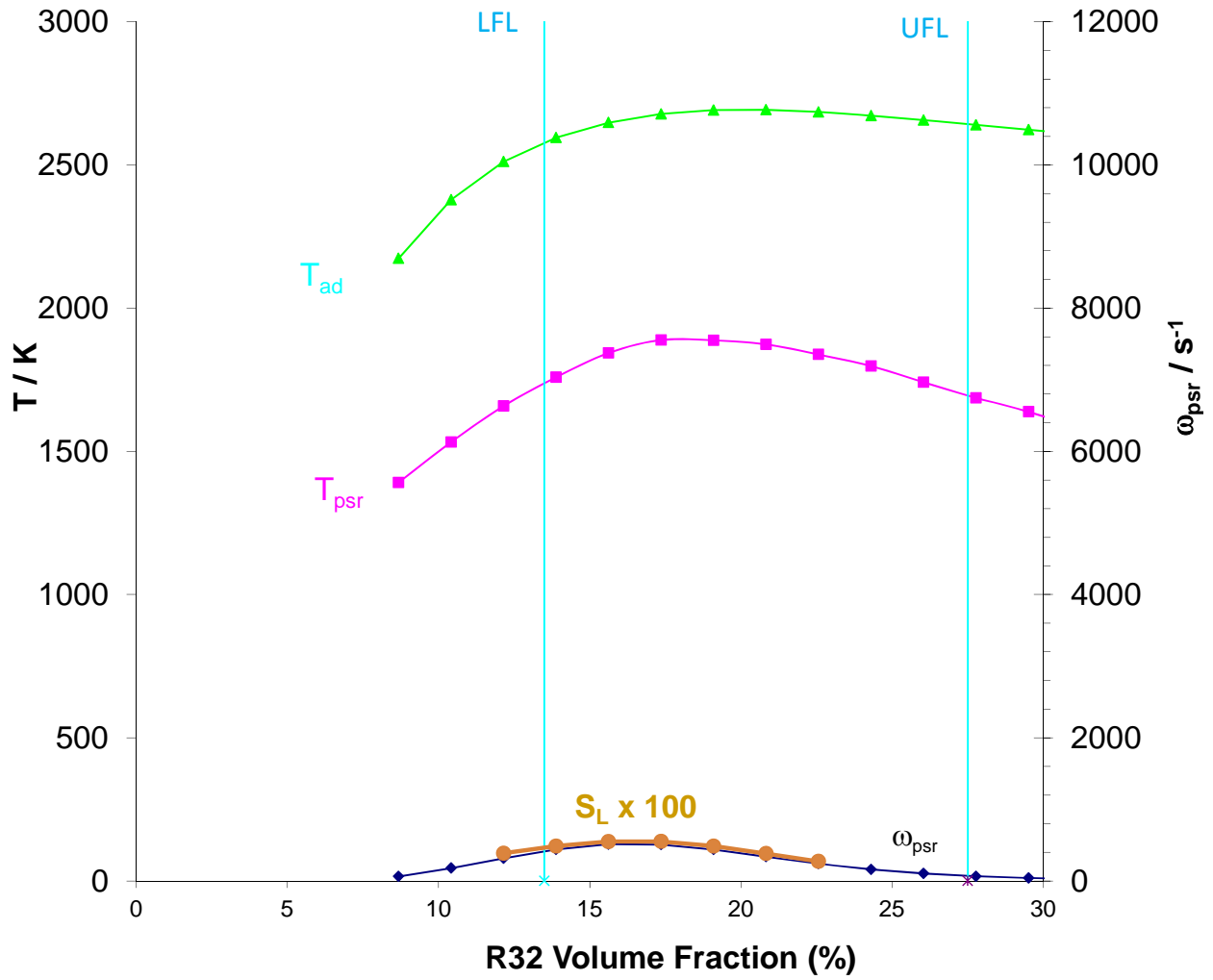


Figure 15 - PSR predictions of overall chemical rate ω_{psr} and laminar flame speed S_L (right scale), and equilibrium adiabatic temperature and PSR temperature (left scale) for R32-air mixtures.

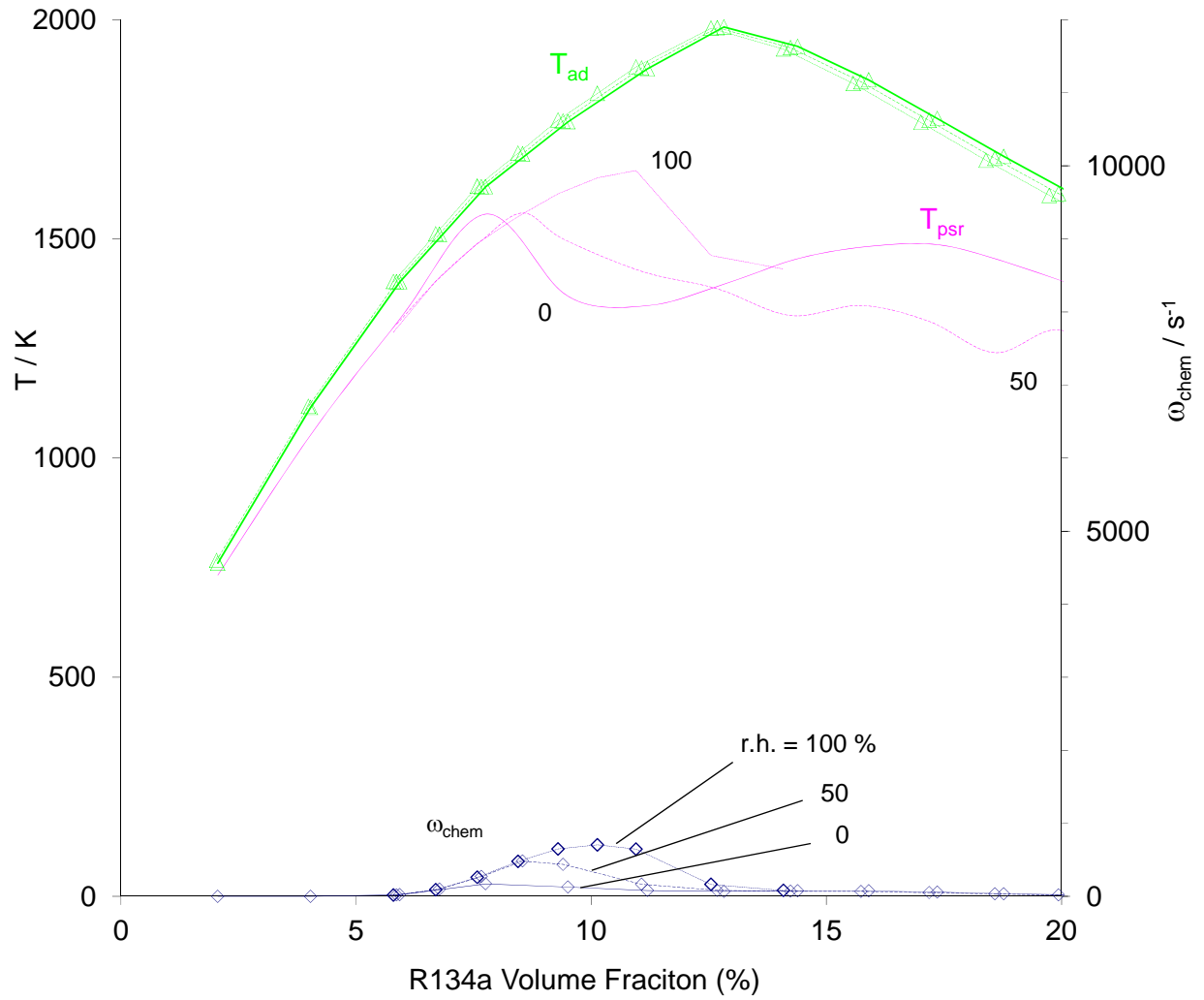


Figure 16 - PSR predictions of overall chemical rate ω_{psr} (right scale), and equilibrium adiabatic temperature T_{ad} and PSR temperature T_{psr} (left scale) for R134a-air mixtures. The three curves for each parameter are for 0 % RH, 50 % RH, and 100 % RH

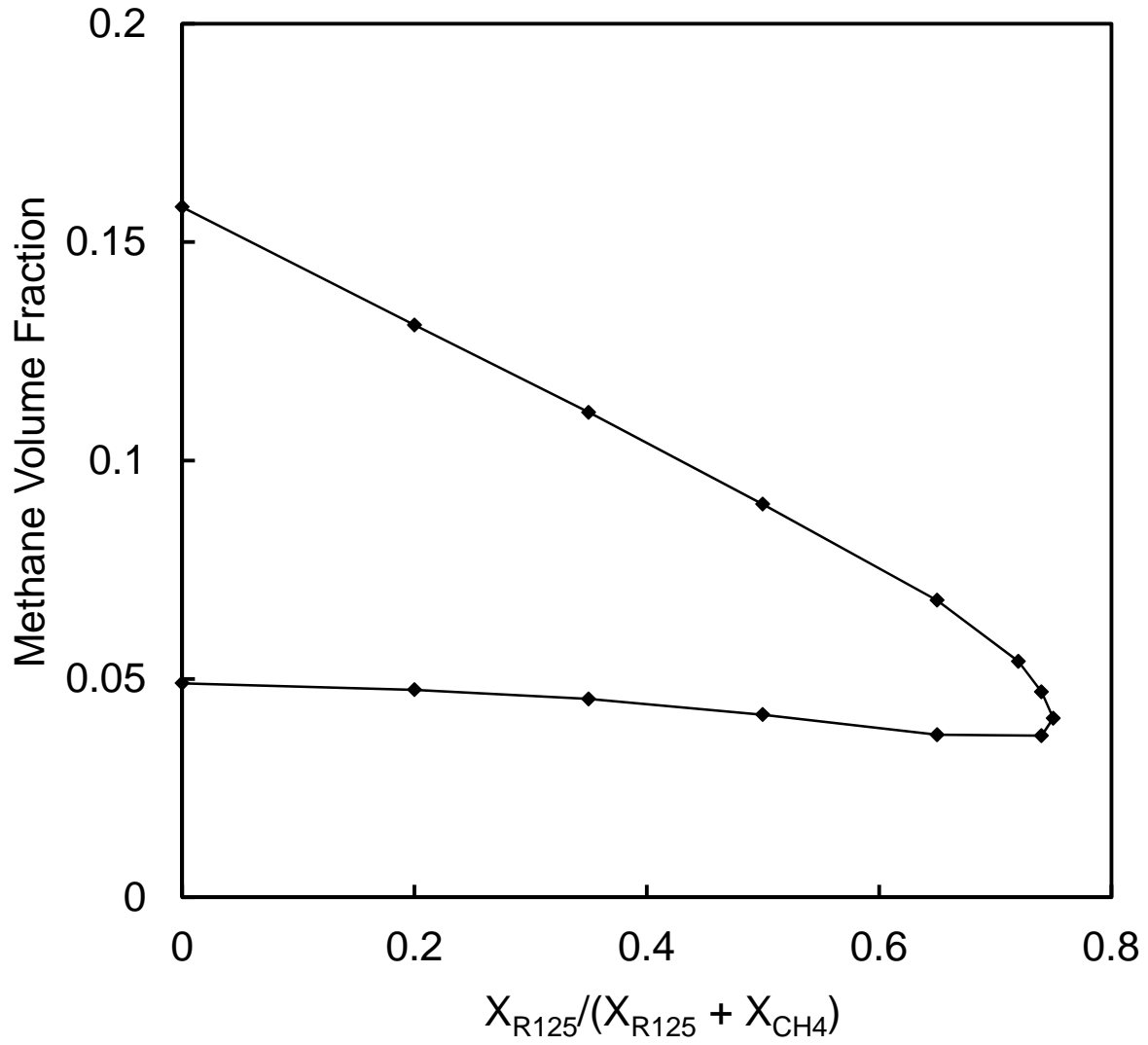


Figure 17 - Flammability envelope for methane air flames with added HFC-125, from ref. [1]

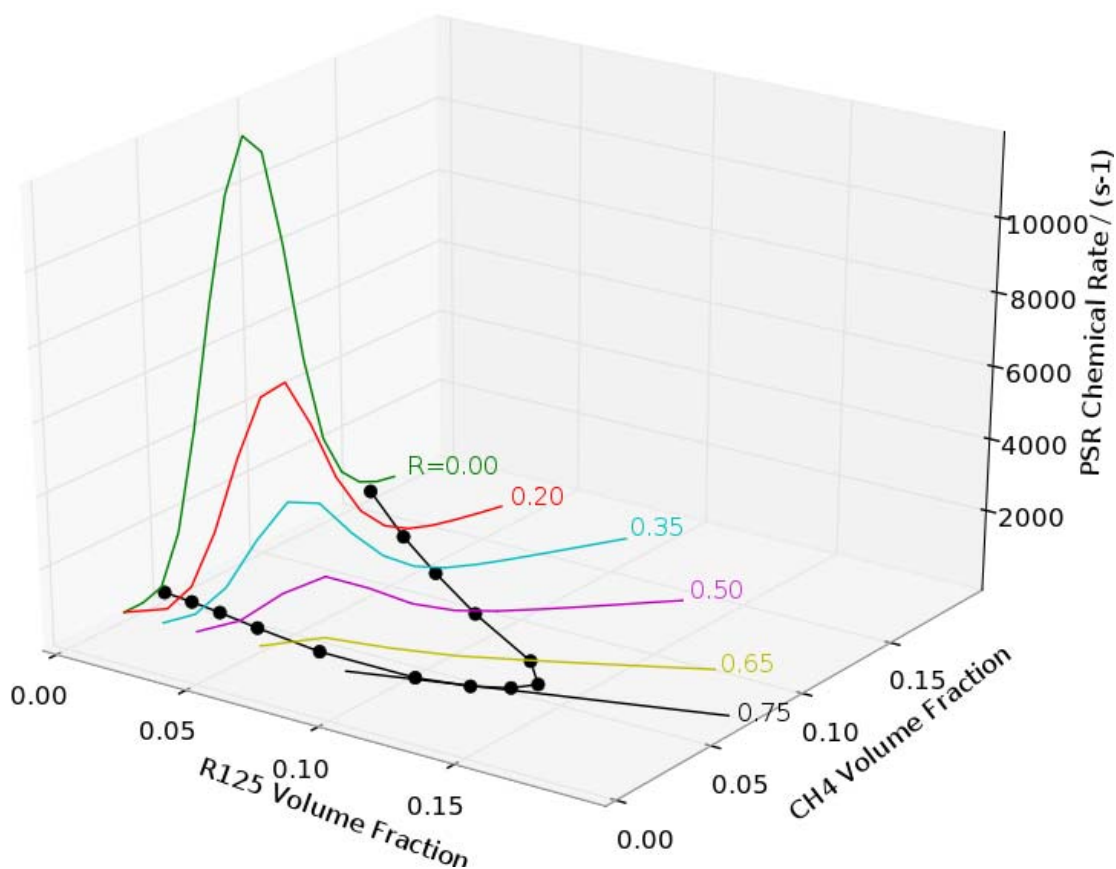


Figure 18 - Overall chemical rate (colored lines, calculated via perfectly-stirred reactor simulations) for CH₄, R-125, and air mixtures, together with experimental data of Kondo et al. [1] (black dots and black line). $R = X_{R125} / (X_{R125} + X_{CH4})$.

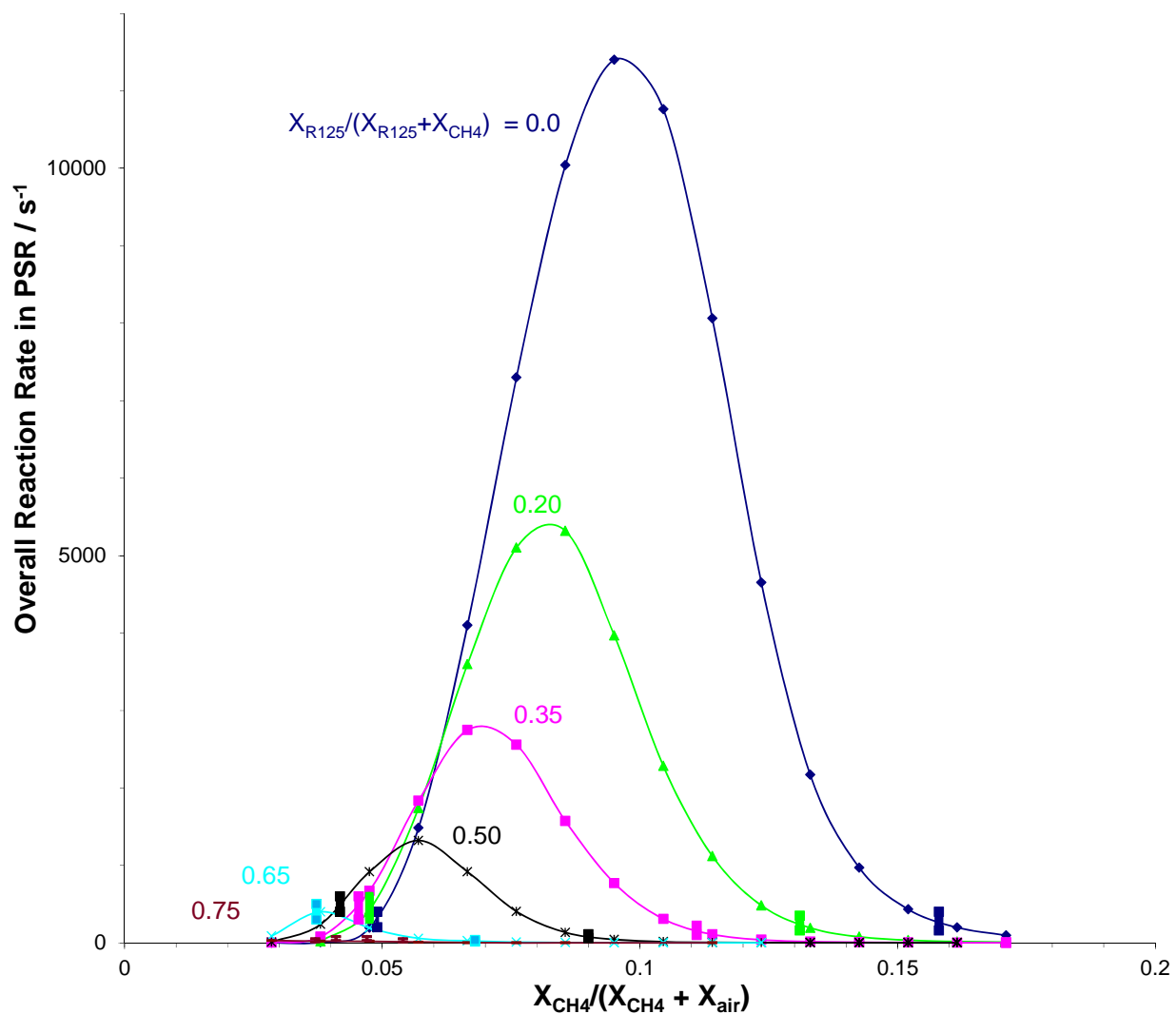


Figure 19 - Overall chemical rate (lines, calculated via perfectly-stirred reactor simulations) for CH₄, R-125, and air mixtures, together with flammability limit data of Kondo et al. [1] (indicated by the solid tick marks near the base of the curves).

APPENDIX I - Japanese High Pressure Gas Law (translation)

Japanese High Pressure Gas Law (translation)

7 Hermetically sealed test pressure

For cryogenic vessels and low-temperature vessels, a pressure of 1.1 times the maximum filling pressure; for vessels filled with acetylene gas, a pressure of 1.8 times the maximum filling pressure; and for other vessels, the maximum filling pressure (Ordinance 29, 1980, part amended)

8 Flammable gases

Acetylene, ammonia, carbon monoxide, ethane, ethylene, vinyl chloride, chloromethane, ethylene oxide, hydrogen cyanide, cyclopropane, hydrogen, trimethylamine, butadiene, butane, butylene, propane, propylene, methane, monomethylamine, methyl ether, hydrogen sulfide, and other gases that correspond to either i) or ii) below (Ordinance 29, 1980, part amended)

i) Having a lower explosion limit (referring to the explosion limit when mixed with air. The same definition is used hereinbelow) of 10 percent or less

ii) Having a difference of 20 percent or more between the upper and lower explosion limits

9 Toxic gases

Sulfur dioxide gas, ammonia, carbon monoxide, chlorine, chloromethane, ethylene oxide, hydrogen cyanide, trimethylamine, monomethylamine, hydrogen sulfide and other gases whose permissible concentration volume is 200/1,000,000 or less (Ordinance 29, 1980, part amended)

Methods for Measuring the Explosion Limits of Flammable Gases

Notification is hereby given that, as per the appendix hereto, methods have been established for measuring the explosion limits mentioned in i) and ii) of the General High-Pressure Gas Safety Regulations, Article 2, Section 1.

The reasons for establishing this standard are as follows.

Article 2, Section 1 of said Safety Regulations defines a flammable gas as "i) Having a lower explosion limit of 10 percent or less, or ii) having a difference of 20 percent or more between the upper and lower explosion limits", but no standard currently exists for the measurement method, with various methods being used. Furthermore, values measured using different measurement methods do not necessarily correspond, and in certain situations a significant disparity can arise. There is thus the danger that problems may arise in relation to whether or not an aerosol propellant or the like, for example, falls within the definition of a flammable gas.

The purpose is thus to standardize the measurement method, by selecting from these various measurement methods the methods described in the appendix, which are currently thought to be the most reliable and most widely used, and further to ensure reproducibility and repeatability of the measured values by standardizing the measurement device, method of operation, calculation method and the like.

This proposal was drafted by preparing a first draft which took account of the opinions of several specialists, including the Government Chemical Industrial Research Institute, Tokyo, then presenting this first draft to related industries (approximately ten organizations) for opinions, and finally making necessary revisions.

It should be noted that the intention is for this standard to be used if JIS Standards or the like are established in the future.

(Appendix)

Standard methods of measuring explosion limits

The methods of measuring the explosion limits mentioned in i) and ii) of the General High-Pressure Gas Safety Regulations, Article 2, Section 1 shall be as follows.

1 Selection of measurement method

To measure the explosion limits of flammable gas or vapor (referred to hereinafter simply as 'gas'), Method A shall be used for gases whose molecules contain halogen, or gases comprising gases whose molecules contain halogen, mixed with other gases (excluding air or oxygen), and Method B shall be used for other gases.

2 Method of measurement

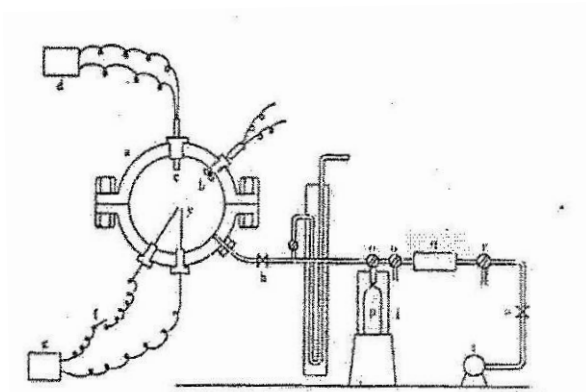
(1) Method A

1. Measurement device

A device such as that shown in Figure 1 shall be used.

Figure 1 Explosion limit measurement device (Method A)

- a: Explosion vessel
- b: Electromagnetic agitator
- c: Thermocouple
- d: mV meter
- f: Switch
- g: Power supply
- h,s: Shutoff valves
- i: Warm water (or oil) bath
- k: Mercury manometer
- o, o': 3-way valves for introduction of samples
- p: Sample vessel
- q: Drying tube
- r: 3-way valve for introduction of air
- t: Vacuum pump
- y: Ignition electrode



(i) Explosion vessel (a)

Shall be a spherical vessel having a capacity of approximately 2 liters, able to withstand an explosive pressure of at least 10kg/cm.

(ii) Ignition device

A platinum wire (diameter 0.3mm, length 20mm) shall be brazed to an electrode (y) which is inserted into the central portion of the vessel, and which is connected to a 100 volt alternating current power supply (g).

(iii) Explosion temperature measuring device

A chromel-alumel thermocouple (c) (sheath cap type, diameter approximately 1mm) shall be mounted inside the vessel, and connected to a full-scale 5mV millivolt recording meter (d).

2. Operation

(i) The entire system within the device is evacuated using a vacuum pump (t).

(ii) The sample gas is introduced into the vessel (a) by opening a sample introduction valve (o or o'). The amount introduced is measured using a mercury manometer (k).

Note: With liquefied gases comprising a mixture of two or more gases, to measure the explosion limits of the composition as exhibited in the liquefied state, a sample is collected in accordance with JIS K2550 (Method of sampling liquefied petroleum gas); when the sample is introduced into the explosion chamber care should be taken to ensure that the composition of the gas inside the explosion chamber does not differ from the composition of the gas in the liquefied state, for example by vaporizing all of the liquefied gas within the sample vessel (p) (such that no liquefied gas remains).

(iii) Air is introduced by opening the air introduction valve (r) until the pressure inside the explosion vessel (a) reaches atmospheric pressure.

(iv) The gas inside the explosion vessel (a) is mixed sufficiently using an electromagnetic agitator (b) to achieve a uniform concentration.

(v) After closing the valve (h), the ignition device switch (f) is turned on, causing the platinum wire to melt and thereby generating a spark.

(vi) If it is determined, by means of the temperature change within the explosion vessel (a), that the gas therein has ignited, then an explosion is deemed to have occurred.

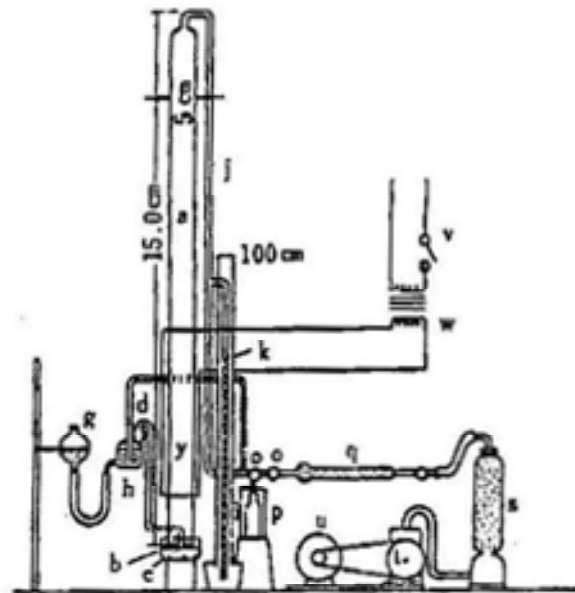
(2) Method B

1. Measurement device

A device such as that shown in Figure 2 shall be used.

Figure 2 Explosion limit measurement device (Method B)

- a: Explosion tube
- b: Glass plate
- c: Mercury bath
- d: Non-return device
- g: Mercury reservoir
- h: Mercury input pump
- i: Warm water (or oil) bath
- h: Manometer
- p: Sample vessel
- q,s: Drying vessels
- t: Vacuum pump
- u: Motor
- v: Switch
- w: Neon transformer
- y: Discharge gap



(i) Explosion tube (a)

Comprises a hard glass tube of internal diameter 5cm and length 150cm, the lower end of which is closed by means of a

ground glass joint, using a lid comprising a glass plate (b), and hermetically sealed by immersion in a mercury bath (c).

(ii) Ignition device

A spark discharge electrode (y) having a gap of approximately 3mm is mounted in the lower portion of the explosion tube, and is connected to a neon transformer (w) which generates a voltage of at least 12 kV.

2. Operation

(i) The entire system within the device is evacuated by operating a vacuum pump (t).

(ii) The sample gas is introduced into the explosion tube (a) by opening a sample introduction valve (o or o'). The amount introduced is measured using a mercury manometer (k).

(iii) Air is introduced via a drying tube (q) until the pressure inside the tube (a) reaches atmospheric pressure.

(iv) The gas within the tube is agitated by raising and lowering a mercury reservoir (g) repeatedly for a period of 10 to 30 minutes to achieve a uniform concentration. Alternatively an electromagnetic agitator or the like may be used.

(v) The mercury bath (c) is lowered and the glass plate (b) is removed, immediately after which the switch (v) is operated, generating a spark discharge at the electrode (y).

(vi) At this time, the flame generated at the ignition location rises up the tube, and an explosion is deemed to have occurred if the flame is observed to have reached the top of the tube.

Note: Propagation of the flame should be observed in a darkened place. If observation is difficult even in a darkened place, then confirmation shall be performed by mounting in the upper portion of the explosion tube the same type of explosion temperature measuring device as in 2-(1)-1-(iii).

3 Determining explosion limits

(1) Upper explosion limit

1. Tests are performed using various different concentrations in the vicinity of the concentration assumed to be the upper

explosion limit (at least two tests each without the occurrence of an explosion and with the occurrence of an explosion); the lowest gas concentration at which an explosion does not occur is defined as V_n (volume %), and the highest gas concentration at which an explosion does occur is defined as V_i (volume %).

2. The upper explosion limit is defined as the value obtained by calculation using the following formula.

$$\text{Upper explosion limit } E_v \text{ (volume \%)} = (V_n + V_i) / 2$$

Provided that V_n and V_i are sufficiently close together that both of the following two formulae are satisfied:

$$\begin{aligned} V_n - V_i &< 3 \text{ (\%)} \\ (V_n - V_i) / V_i &< 0.1 \end{aligned}$$

(2) Lower explosion limit

1. Tests are performed using various different concentrations in the vicinity of the concentration assumed to be the lower explosion limit (at least two tests each without the occurrence of an explosion and with the occurrence of an explosion); the lowest gas concentration at which an explosion does occur is defined as L_i (volume %), and the highest gas concentration at which an explosion does not occur is defined as L_n (volume %).

2. The lower explosion limit is defined as the value obtained by calculation using the following formula.

$$\text{Lower explosion limit } E_l \text{ (volume \%)} = (L_i + L_n) / 2$$

Provided that L_i and L_n are sufficiently close together that both of the following two formulae are satisfied:

$$\begin{aligned} L_i - L_n &< 3 \text{ (\%)} \\ (L_i - L_n) / L_n &< 0.1 \end{aligned}$$

APPENDIX II - Standard Operating Procedure for 2-L Chamber

Nominal Procedure

1. Verify desired initial conditions of test:
 - pressure
 - temperature
 - composition (fuel, air, humidity)
 - ignition type (wire or spark)
 - sensor type (dP/dt, T, or both)
 - locate and get ready to fill in lab notebook book.
2. Verify that vent is working (Magnehelic gage at 0.2 in. water, vent sucking air, exhaust fans audible).
3. Verify igniter power off.
4. Turn N₂, reactant air, and reactant fuel bottles on.
5. Pressure purge chamber (see below).
6. Pressure test chamber and pressure relief valve (see below).
7. Vacuum vent chamber (see below).
8. Install Platinum igniter (see below).
9. Vacuum test chamber (see below).
10. Vacuum vent chamber (see below).
11. Flush chamber with reactant air:
 - a. Verify all chamber valves are closed.
 - b. Open purge vent valve.
 - c. Set 5-way valve to air.
 - d. Set secondary chamber valve to 5-way.
 - e. Open main chamber fill valve.
 - f. Flush for 1 min.
 - g. Close main chamber fill valve.
 - h. Close secondary chamber fill valve.
 - i. Close purge vent valve.
12. Add test air to chamber:
 - a. Verify chamber pressure is equal to ambient by opening the purge vent valve.
 - b. Open the Omega pressure sensor valve.
 - c. Close purge valve.
 - d. Set 5-way valve to air.
 - e. Set secondary chamber fill valve to 5-way.
 - f. Using the main chamber fill valve to establish the initial air pressure in the chamber to 800 Torr.
 - g. Close main chamber fill valve.
 - h. Set 5-way valve to fill line vac.
 - i. Open main chamber fill valve to establish air pressure at the desired condition specified on the run sheet.
 - j. Close main chamber fill valve

13. Purge fill lines:
 - a. Verify main chamber fill valve closed.
 - b. Set 5-way valve to fill line vac.
 - c. Set secondary chamber fill valve to 5-way.
 - d. Wait 10 sec.
14. Purge fill lines with agent.
 - a. Select agent with fuel selection valve.
 - b. Set 5-way valve to fuel, to the fill manifold with agent.
 - c. Switch 5-way valve back and forth between fuel and fill line vac 5 times while waiting 10 sec each time when the valve is set to fill line vac.
 - d. End with the 5-way valve on fuel.
 - e. Record chamber pressure (air only).
15. Add agent to chamber:
 - a. Open the main chamber valve; establish the final pressure in chamber (approximately 760 Torr).
 - b. Wait 5 mins, then record final fill pressure.
 - c. Verify main chamber fill valve is closed.
 - d. Set 5-way valve to fill line vac.
 - e. Set 5-way valve to air.
16. Close Omega pressure sensor valve.
17. Plug ignitor into Variac.
18. Verify N₂ inlet valve, Omega pressure gage valve, purge vent valve, main chamber fill valve, all closed.
19. Verify thermocouples working.
20. Verify PCB pressure gage working.
21. Ear muffs on.
22. Start Labview vi.
23. Flip the Variac ignition switch manually for 2 seconds and then switch it off.
24. Unplug ignitor plug from Variac.
25. Open the N₂ inlet valve.
26. Open the Purge vent valve.
27. Wait 1 min.
28. Close N₂ inlet valve.
29. Close Purge vent valve.
30. Test Variac with lamp.
31. Pressure purge chamber (see below).
32. Vacuum vent chamber (see below).
33. Pressure purge chamber (see below).
34. Vacuum vent chamber (see below).
35. Verify data is collected.
36. Shut down DAS.
37. Shut all gas valves on supply gases.

Pressure Purge Chamber

1. Verify all chamber valves closed.
2. Open the Air inlet valve.
3. Open purge vent valve.
4. Purge for 2 minutes.
5. Close air inlet valve.
6. Close purge vent valve.

Pressure test chamber and pressure release valve.

1. Verify all valves closed.
2. Set N₂ regulator to 170 psig (nominal).
3. Open N₂ inlet valve.
4. Verify the pressure relief valve opens.
5. Close N₂ inlet valve.
6. Set regulator to 160 psig (nominal).
7. Open N₂ inlet valve.
8. Wait 2 mins and verify that the chamber pressure has not decreased by more than 2 psig.
9. Close N₂ inlet valve.
10. Open the purge vent valve and vent chamber to ambient.
11. Close all valves.

Vacuum Vent Chamber

1. Verify chamber pressure is at ambient or lower
2. Open Omega pressure gage valve.
3. Verify purge vent valve closed
4. Set secondary chamber fill valve to chamber vac.
5. Open main chamber fill valve.
6. Wait for the chamber to reach approximately 100 Torr on Omega readout.
7. Maintain vacuum for 5 minutes.
8. Close main chamber fill valve.
9. Set 5-way valve to air
10. Set secondary fill valve to 5-way
11. Open main chamber fill valve and slowly bring pressure to ambient.
12. Close main chamber fill valve.
13. Close secondary chamber fill valve.

Vacuum test chamber:

1. Verify chamber pressure is at ambient or lower.
2. Open the Omega pressure gage valve.
3. Set the secondary chamber fill valve to chamber vac.
4. Open main chamber fill valve.

5. Wait for the chamber to reach approximately 100 Torr.
6. Close the main chamber fill valve and wait 2 mins. Verify that chamber pressure has not increased by more than 20 Torr.
7. Set 5-way valve to air
8. Set secondary fill valve to 5-way
9. Open main chamber fill valve and slowly bring pressure to ambient.
10. Close main chamber fill valve.
11. Close secondary chamber fill valve.

Install Platinum Igniter

1. Verify chamber at ambient laboratory pressure (open purge vent valve, and close.).
2. Verify igniter power off.
3. Remove igniter plug from Variac outlet.
4. Put on Nitrile gloves.
5. Remove igniter assembly.
6. Remove old igniter Platinum wire from assembly and discard.
7. Install new Platinum wire in assembly.
8. Install igniter assembly.
9. Discard Nitrile gloves.
10. Test resistance across igniter leads at plug, and record.
11. Check for resistance > 1000 ohms from either lead of igniter to chamber body.

Safety Considerations:

1. When removing igniter, be sure igniter is un-plugged and Variac is powered down.
2. Wear ear muffs when igniting the combustible mixture.
3. In the event of a power failure, water leak in the lab, emergency evacuation, etc., shut off all valves and leave the room.
4. The chamber is heavy and is a lifting/dropping hazard. For lifting, use two people when appropriate. Routine operation of the 2 L chamber does not require removal of the top half. When it does, remove the top fitting (1/2" NPT) and insert the lifting handle to make handling easier, and wear leather gloves.
5. If a supply line fails during the fill procedure, shut off the gas supply to that line.

Emergency Shutdown

1. Each experimental run test time is less than a second, and after an experiment run, there are no hazards associated with this tool operating unattended; therefore, the instrument itself it does not need to be shutdown in an emergency (see #2 below).
2. In an event the tool must be shut down immediately, shut all gas-supply valves and turn off igniter power supply.

3. If an alarm occurs for fire, shelter in place, etc., shut off gases at the supply bottle and immediately leave the room. It is not necessary to shutdown the instrument. If the emergency is in the lab, leave immediately and contact NIST emergency operator at extension x2222.

APPENDIX III - Raw data for flammability tests with 2-L chamber

Agent	Run Date	Run Number	Igniter Type	Agent Partial Pressure (%)	Peak Temperature Rise (K)	Peak Pressure Rise (bar)	Relative Humidity (%)
Air	6/16/2011	5	Pt	0	10.3	0.07377	
N2	6/16/2011	4	Pt	0	3.9	0.07839	
CH4	6/16/2011	1	Pt	4.5	7	0.034474	
	6/23/2011	2	Pt	4.65	81	0.337843	
	6/16/2011	2	Pt	4.77	88	0.344738	
	6/14/2011	4	Pt	4.8	157	0.689476	
	6/16/2011	3	Pt	4.81	142	0.758423	
	6/23/2011	1	Pt	4.883	145	0.606739	
	6/14/2011	3	Pt	4.9	114	0.413685	
	6/14/2011	2	Pt	5	210	1.378951	
	6/17/2011	1	Pt	6	265	3.792117	
	6/23/2011	3	Pt	15	316	2.661376	
	6/23/2011	4	Pt	17	207	0.680513	
	6/23/2011	5	Pt	18	71	0.27579	
	6/23/2011	6	Pt	19	73.5	0.238559	
	6/28/2011	1	Pt	20	67.8	0.205464	1.2
	6/28/2011	2	Pt	22	59.3	0.19719	1.8
	6/28/2011	3	Pt	25	48.2	0.21029	1.8
	9/23/2011	5	Cu	4.7	1.6	0.008963	
	9/23/2011	4	Cu	5.0	164.6	0.623976	
	9/23/2011	3	Cu	14	298.3	3.27501	
	9/23/2011	2	Cu	16	1.76	0.001103	
	9/23/2011	1	Cu	19	3.9	0.002895	
R32	7/7/2011	3	Pt	11	1.5	0	1.2
	7/7/2011	2	Pt	12	243	0.827371	1.8
	7/7/2011	1	Pt	13	346	2.688955	2.1
	7/1/2011	2	Pt	14	375	3.998959	1.0
	7/1/2011	1	Pt	15.6	400	0	1.3
	7/7/2011	6	Pt	26	313	3.240536	1.1
	7/7/2011	4	Pt	27.64	195	1.241056	1.2
	7/7/2011	7	Pt	29	39.4	0.262001	1.3
	7/7/2011	5	Pt	30	11	0.045505	0.7
1234ZE	7/14/2011	1	Pt	6	17.6	0.075842	1.7
	7/14/2011	7	Pt	6.5	3.3	0.020684	1.1
	7/15/2011	1	Pt	6.75	225	0.85495	1.8
	7/14/2011	2	Pt	7	397	1.413425	1.2
	7/15/2011	3	Pt	8	405	2.640692	1.2
	7/14/2011	5	Pt	9	400	3.309483	1.1
	7/15/2011	4	Pt	10	393	3.199167	1.2
	7/12/2001	1	Pt	11	405	1.792637	1.3
	7/15/2011	5	Pt	11.1	336	2.585534	1.2
	7/14/2011	8	Pt	11.5	350	2.206322	1.2
	7/15/2011	2	Pt	12.25	207	1.234162	1.4
	7/14/2011	3	Pt	13	129	0.661897	1.2

	7/14/2001	4	Pt	14	48	0.262001	1.2
	7/14/2011	6	Pt	15	10.6	0.041369	1.1
	7/12/2011	2	Pt	30	2	0.020684	1.1
	7/21/2011	2	Cu	8	0.3	0	1.5
	7/21/2011	1	Cu	9	0.3	0	1.5
	7/21/2011	3	Cu	10	0.3	0	1.5
R134a	7/21/2011	3	Pt	5	1.7	0.01379	1.1
	7/21/2011	1	Pt	6	9.8	0.048263	1.1
	7/21/2011	2	Pt	8	5	0.027579	1.2
	7/22/2011	1	Pt	12	12	0.103421	2.1
	7/25/2011	3	Pt	12	21.6	0.113074	2.5
	7/25/2011	1	Pt	8.6	17.6	0.103421	57.8
	7/25/2011	2	Pt	12	1.3	0.01379	56.8